Geochemistry, Geophysics, Geosystems®

AGU ADVANCING EARTH AND SPACE SCIENCES

RESEARCH ARTICLE
10.1029/2023GC011147

Organic Phases in Bivalve (*Arctica Islandica*) Shells: Their Bulk and Amino Acid Nitrogen Stable Isotope Compositions

Qian Huang[1], Oluwatoosin B. A. Agbaje[2], Martina Conti[3], and Bernd R. Schöne[1]

[1]Institute of Geosciences, University of Mainz, Mainz, Germany, [2]Section for GeoGenetics, Faculty of Health and Medical Sciences, Globe Institute, Copenhagen University, København, Denmark, [3]Department of Chemistry, University of York, York, UK

Key Points:

- Organic phases in modern bivalve shells carry different nitrogen isotope compositions
- The amino acid composition differed between total organics and intra-organics, resulting in different nitrogen isotope data

Supporting Information:

Supporting Information may be found in the online version of this article.

Correspondence to:

Q. Huang,
qhuang01@uni-mainz.de

Citation:

Huang, Q., Agbaje, O. B. A., Conti, M., & Schöne, B. R. (2023). Organic phases in bivalve (*Arctica islandica*) shells: Their bulk and amino acid nitrogen stable isotope compositions. *Geochemistry, Geophysics, Geosystems*, *24*, e2023GC011147. https://doi.org/10.1029/2023GC011147

Received 24 JUL 2023
Accepted 4 OCT 2023

Author Contributions:

Conceptualization: Qian Huang, Bernd R. Schöne
Data curation: Qian Huang
Formal analysis: Qian Huang
Funding acquisition: Bernd R. Schöne
Methodology: Qian Huang, Oluwatoosin B. A. Agbaje, Martina Conti
Resources: Bernd R. Schöne
Validation: Qian Huang, Oluwatoosin B. A. Agbaje, Martina Conti
Visualization: Qian Huang
Writing – original draft: Qian Huang
Writing – review & editing: Oluwatoosin B. A. Agbaje, Martina Conti, Bernd R. Schöne

Abstract The stable nitrogen isotope composition of bivalve shell organics serves as a proxy for nitrogen fluxes in modern and past ecosystems. An essential prerequisite to reconstruct environmental variables from $\delta^{15}N$ values of bivalve shells is to understand if pristine isotope signals can be retrieved from shell organics after sample pretreatment. $\delta^{15}N$ analyses of fossil shells should be limited to the intra-crystalline organic matrix (intra-OM), which is trapped within biomineral units and less likely contaminated or diagenetically overprinted than inter-crystalline organics (inter-OM). However, it remains unclear whether the different shell organic phases (insoluble/soluble inter-OM, intra-OM) are isotopically distinct and whether $\delta^{15}N$ values of intra-OM agree with those of bulk organic matter. These questions were tackled by applying different solvents (H_2O, HCl, H_2O_2, NaOCl) to homogenized shell powder of a modern *Arctica islandica*. Milli-Q water did not alter bulk $\delta^{15}N$ values indicating the dissolution of the inter-OM was negligible. Acid-extracted intra-OM exhibited a larger isotope variation within replicates and showed a minor but significant fractionation in bulk $\delta^{15}N$ values related to the loss of acid-soluble components. Compared to H_2O_2, NaOCl oxidative treatment was more effective in cleaning inter-OM and produced reliable bulk and amino acid (AA)-specific $\delta^{15}N$ data of intra-OM. Furthermore, differences in the relative abundance and $\delta^{15}N$ values of individual AAs suggested that the N isotope composition is not uniform within shells, and the N-bearing content and AA composition differ between organic phases. Future studies should test the capability of bulk and CSIA-AA $\delta^{15}N$ proxies in fossil shells as paleoenvironmental archives.

Plain Language Summary The nitrogen isotope ratio ($^{15}N/^{14}N$) of organics embedded in bivalve shells can be used to understand biogeochemical processes in the environment. When applying chemical solvents to clean the shells, some organic phases are inevitably lost. To evaluate the potential effects of chemical cleanings on nitrogen isotope composition ($\delta^{15}N$) in shell organics, we applied various solvents to modern shell samples. Most of the shell organic phases carry specific distinct amino acid (AA) compositions and therefore have different nitrogen isotope compositions. These results imply that the nitrogen-bearing contents (such as AA) and their isotope compositions are not uniform within shells. Specifically, we compared the organics entrapped inside crystals (intra-OM) with the total shell organics (raw-OM). The offsets in bulk $\delta^{15}N$ data between the two phases were mainly driven by the difference in AA proportions, while little differences were observed in $\delta^{15}N$ values of AA. Technically, using raw shells without chemical pretreatment and using a bleaching protocol is suitable for raw-OM and intra-OM, respectively, to obtain the bulk and AA-specific $\delta^{15}N$ data. These findings indicate that raw-OM is sufficient for bulk and AA-specific $\delta^{15}N$ analyses in modern bivalve shells for environmental reconstructions and provide a framework to study the fossil shells.

1. Introduction

Bivalve shells are a powerful biogenic archive for reconstructing past environmental and ecological conditions in aquatic settings (Rhoads & Lutz, 1980; Richardson, 2001; Steinhardt et al., 2016). Many bivalves are sessile residents that filter particulate organic matter (OM) from the ambient water and integrate such resources into their soft tissues and shell (Newell, 2004; O'Donnell et al., 2003). Unlike the soft tissues, shell OM is not continuously renewed and turned over by the metabolism but preserves temporally constrained information on changes in the food sources (Graniero et al., 2016; O'Donnell et al., 2003; Vokhshoori et al., 2022), that is, digested algae and bacteria as well as organic detritus deriving from decayed organisms belonging to higher trophic positions. Stable nitrogen isotope ($\delta^{15}N$) values of bulk tissues (bulk stable isotope analysis, BSIA) [BSIA-$\delta^{15}N$] can provide

important insights into the nitrogen sources (dissolved inorganic nitrogen, DIN) and the trophic position (TP) of organisms (Fry, 2006) with the underlying principals that (a) $\delta^{15}N_{DIN}$ values are reflected in primary producers (the so-called nitrogen isotope baseline) (Post, 2002) and (b) an average increase of 3–4 ‰ occurs during each trophic transfer (Deniro & Epstein, 1981; Minagawa & Wada, 1984). BSIA-$\delta^{15}N$ values of shell OM extracted from whole valves, shell fragments or individual annual growth increments can provide information on natural variations of the nitrogen isotope baseline in time and space (e.g., Graniero et al., 2021; Schöne & Huang, 2021; Vokhshoori et al., 2022) as well as nutrient and pollutant loadings affecting the aquatic biogeochemistry (e.g., Black et al., 2017; Kovacs et al., 2010; Oczkowski et al., 2016).

Compound-specific stable isotope analysis (CSIA) of individual amino acids (AAs) [CSIA-$\delta^{15}N_{AA}$] is a technique that provides much more detailed information on the consumer physiology (Fantle et al., 1999; McClelland & Montoya, 2002; Popp et al., 2007). This method is based on the observation that AAs are metabolized in different ways associated with differences in nitrogen isotope fractionation. From resources to consumers, the so-called source AAs experience only little nitrogen isotopic change (Chikaraishi et al., 2007; Fantle et al., 1999; McClelland & Montoya, 2002), but trophic AAs become enriched in ^{15}N (Chikaraishi et al., 2007; Macko et al., 1986; McClelland & Montoya, 2002) leading to higher $\delta^{15}N$ values. While BSIA-$\delta^{15}N$ have limitations in the food web reconstruction, for instance, the large variability in isotope values of primary producers (e.g., Vizzini & Mazzola, 2003) and isotopic fractionations through the trophic transfer (e.g., Caut et al., 2009), CSIA-$\delta^{15}N_{AA}$ enables more precise estimates of the nitrogen isotope baseline and the TP (see review by Ohkouchi et al. (2017)). Although CSIA-$\delta^{15}N_{AA}$ of shell organics is still in its infancy, vast potential has been revealed by using this technique to reconstruct organic sources and the nitrogen isotope baseline back in time (Ellis, 2012; Misarti et al., 2017; Vokhshoori et al., 2022) at an unprecedented temporal resolution (Huang, Wu, & Schöne, 2023).

An essential prerequisite to reliably reconstruct environmental variables from $\delta^{15}N$ values (both BSIA and CSIA-AA) of bivalve shells is to understand if pristine isotope signals can be retrieved from shell organics after sample preparation. To obtain such data often requires several cleaning and pretreatment steps prior to the measurements. For example, the low nitrogen content in shells, even in modern and diagenetically unaltered bivalves, hampers the reliability of BSIA-$\delta^{15}N$ data (Carmichael et al., 2008; Darrow et al., 2017), given that the overwhelmingly abundant carbonate matrix can cause an incomplete combustion and can overload the isotope ratio mass spectrometer (IRMS). Particular instrumental settings of the nano-EA (elemental analyzer) are hence required, for example, auto-sampler evacuation, reduction of quartz reactors, and potentially, a special CO_2 trapping system (Polissar et al., 2009; Schöne & Huang, 2021; Versteegh et al., 2011), which can be practically challenging and cost higher analytically. As an alternative, the shell can be dissolved in acid (usually diluted HCl) and the acid-insoluble remainder can be collected ("acid washing" procedure e.g., Kovacs et al., 2010; Oczkowski et al., 2016; Watanabe et al., 2009). However, acid washing can (Carmichael et al., 2008; Das et al., 2021) or may not (Darrow et al., 2017; Pape et al., 2018) influence the nitrogen isotope compositions of shell organics, or in a broader sense, samples with high content of carbonates (see review by Schlacher & Connolly, 2014). The issue has been long recognized by ecologists, yet the discussion has been equivocal - the fractionation is at times positive or negative and inconsistent in magnitude and direction, calling for the understanding of causes (Schlacher & Connolly, 2014). In case of shells, multiple different processes can induce changes of the isotope composition, for example, the loss of soluble components, kinetic fractionation in the insoluble phases, or volatilization of nitrogenous compounds, which remains to be identified. Similar to acid washing, the procedure of rinsing shells in MilliQ water combined with ultrasonication, which was sometimes used to remove potential contaminants during the sample handling (e.g., Milano et al., 2020), can likewise be problematic as it can remove the interstitial soluble substances.

Shell organics (raw-OM) consist of inter- and intra-crystalline fractions (inter- and intra-OM). The inter-crystalline phase (i.e., organics located in interstitial spaces between individual biomineral units) forms a framework for the deposition of calcium carbonate, while the intra-crystalline phase becomes entrapped within the individual biomineral units during the shell formation (Mann, 2001; Marin et al., 2007; Meldrum & Cölfen, 2008). Given that inter- and intra-OM differ by formation pathways (Addadi et al., 2006), these two organic pools can vary fundamentally in their macromolecular composition, for example, protein species and hence the relative abundance of AAs (Nudelman et al., 2007). For instance, distinct AA compositions were found between intra-OM and raw-OM in some bivalves with nacroprismatic shells, with a higher proportion of acidic hydrophilic moieties (e.g., enriched in aspartic acid) occurring in the intra-crystalline phase (Marin & Luquet, 2004; Penkman et al., 2008; Pereira-Mouriès et al., 2002). The AA composition of the organic pool can influence its

nitrogen isotope value because $\delta^{15}N$ values vary greatly among different AAs (Hare et al., 1991; McClelland & Montoya, 2002). As such, the nitrogen-bearing component and $\delta^{15}N$ composition of shell organic pools are associated with the shell biomineralization processes, but knowledge on the shell biomineralization is largely limited to nacroprismatic shells (Addadi et al., 2006; Nudelman et al., 2007). Furthermore, in contrast to the inter-OM that is more susceptible to leaching and contamination, the intra-OM of shells is well protected by the biominerals and less prone to diagenesis (Penkman et al., 2008; Sykes et al., 1995), and, as such, could be a more ideal candidate for paleoenvironmental reconstructions. These observations call for the study of potential isotope and compositional differences between shell intra-OM and raw-OM pools in order to explore the full potential of different shell OM substrates as archives for isotope-based geochemical proxies. To extract shell intra-OM, the weakly bound inter-OM needs to be removed by applying an oxidation reagent, such as NaOCl or H_2O_2 (Penkman et al., 2008). Penkman et al. (2008) reported a more effective oxidation of inter-OM by NaOCl than by H_2O_2, although it remains untested to what extent the different oxidation reagents (i.e., NaOCl and H_2O_2) affect the $\delta^{15}N$ values of extracted organics.

As the difference in bulk and AA-specific $\delta^{15}N$ values between shell organic pools and the potential influence of preparation techniques are poorly understood, these uncertainties can lead to significant isotope biases that affect environmental reconstructions and can hinder comparisons among studies. Here, such issues were tackled by testing how different preparation techniques affect the $\delta^{15}N$ values of raw-OM and intra-OM. To this end, homogenized modern shell powder was used from the long-lived bivalve, *Arctica islandica*, a species that has been extensively exploited in sclerochronological studies (Schöne, 2013). Specifically, this study addresses the following aspects. Firstly, to determine the necessity of washing steps for BSIA-$\delta^{15}N$ of shell raw-OM, we assessed if, to which extend, and how acid washing and Milli-Q water washing influence the isotope composition of raw-OM (note, this was not tested for CSIA-$\delta^{15}N_{AA}$, because the pretreatment effects on AA-specific $\delta^{15}N$ of *A. islandica* shells have been examined by Huang, Wu, and Schöne (2023)). Secondly, to obtain reliable $\delta^{15}N$ data from intra-OM (BSIA-$\delta^{15}N$ and CSIA-$\delta^{15}N_{AA}$), the effects of two oxidation reagents (H_2O_2, NaOCl) were explored. Thirdly, the potential differences in bulk and individual AA isotope compositions as well as the relative abundance of AAs between raw-OM and intra-OM pools were examined in order to provide insights into the potential archive substrate and shell biomineralization. The results of the present study can help to improve nitrogen isotope-based environmental reconstructions based on bivalve shells.

2. Materials and Methods

2.1. Sample Material

Three shells of *A. islandica* (ICE12-05-A14, ICE12-05-A13 and ICE12-05-A04, which hereafter are referred to as Shell A, Shell B and Shell C, respectively) were randomly selected from specimens collected alive in NE Iceland (Þistilfjörður, Þórshöfn) in August 2012. Shell height and shell length were measured with a caliper (shell morphology measurement is shown in Data Set S1). Soft tissues were removed immediately after collection and the shells were cleaned and stored in a dark and dry environment. The right valves of the selected shells were physically cleaned with 150 μm Al_2O_3 powder in a "sandblaster" to remove the periostracum, placed in a ziplock bag and crushed with a hammer. Afterward, the shell was rinsed with Milli-Q (MQ) water and dried in an oven at 50°C overnight. The dried shell fragments were ground in a CryoMill (Retsch GmbH Germany) for 10 min, generating homogenized shell powders (>90 wt % of grains with a size of less than 500 μm). All solvents and reagents for sample processing in this study were at or above HPLC grade and all glassware was thoroughly washed in MQ water and combusted at 450°C for 4 hr.

2.2. Extraction of Organic Phases With Different Solvents

One aliquot of the homogenized powder of each valve was used for BSIA-$\delta^{15}N$ and the other aliquot was prepared for AA composition measurements. Each aliquot was assigned to the following treatments: the Control group (no treatment) and powders treated with acid (HCl), MQ water, and oxidation reagents (H_2O_2 or NaOCl). Each of these treatments produced different phases of shell organic matrices (Figure 1). Prior to these treatments, each aliquot was further divided into three sub-aliquots that served as replicates for each treatment group. The protocols for each of the three sub-aliquots are as follows:

1. The **Control** group consisted of the raw organic matrix (raw-OM) from which the shell powders were taken directly for further analyses.

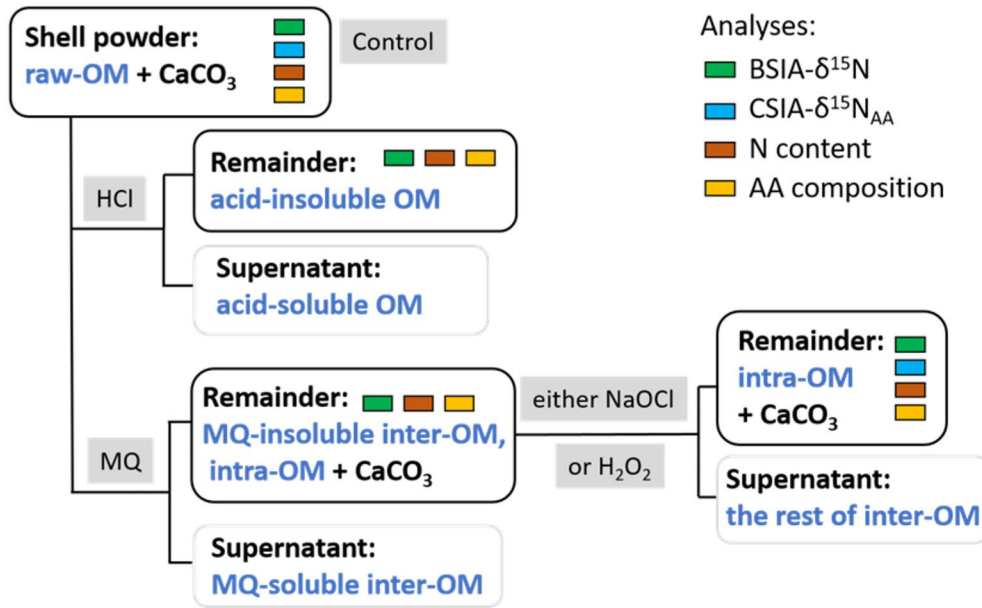

Figure 1. Scheme to illustrate the sample treatment procedure to isolate different phases of shell organic matrices (in blue font). The control group of shell powder underwent no treatment so that the organic matter (OM) was not modified (raw-OM). Shell powders were immersed in different solvents including acid (HCl), MilliQ (MQ) water and two oxidation reagents (H_2O_2, NaOCl). The remaining fractions after centrifugation comprised acid-insoluble OM, MQ-insoluble inter-crystalline organic matter (inter-OM) and intra-crystalline organic matter (intra-OM), respectively. These organic phases were analyzed for bulk stable nitrogen isotope composition (BSIA-$\delta^{15}N$), nitrogen (N) content and amino acid (AA) composition. In addition, raw-OM and intra-OM were measured for the protein AA-specific nitrogen isotope composition (CSIA-$\delta^{15}N_{AA}$).

2. The **HCl** group comprised an acid-insoluble shell matrix. The homogenized shell powders (approx. 250 mg in each sub-aliquot) were weighed into 15 mL polypropylene tubes. 1 mL of 1 N HCl was added slowly to each tube with gentle agitation, and the samples were left to react at room temperature for 5–10 min. This procedure was repeated three times until the bubbling ceased. Then, the samples were centrifuged at 4,500 rpm for 10 min. The supernatant was decanted and the remainders (acid-insoluble phase of OM) were rinsed three times with MQ water, oven-dried at 50°C overnight and stored in a desiccator until further analyses.
3. The **MQ** group was treated by immersing shell powders (approx. 2,500 mg) in 45 mL polypropylene tubes with approx. 35 mL MQ water, treated with ultrasound for 10 min, and left on a shaking table for 48 hr. The samples were then centrifuged at 4,500 rpm for 10 min, and the supernatant was removed by decantation. The remainders, that is, a combination of MQ water-insoluble inter-crystalline and total intra-crystalline organic phases, were oven-dried and stored in a desiccator.
4. To further analyze the intra-crystalline OM, powders (approx. 900 mg in each sub-aliquot) from (3) were immersed in the excessive amount of 12 vol% NaOCl (50 µL per mg of sample) for 48 hr on a shaking table to remove inter-OM from target sample. The NaOCl solution was then discarded after centrifugation (4,500 rpm for 10 min). The remainders were rinsed six times with MQ water, dried at 50°C overnight and stored in a desiccator (the **NaOCl** group).
5. To compare the effect of different oxidization reagents (NaOCl, H_2O_2), approximately 900 mg of shell powders from (3) were treated with excessive 30 vol% H_2O_2 (50 µL per mg of sample) (Penkman et al., 2008). The following extraction steps were the same as for (4) (the **H_2O_2** group).

2.3. Bulk Stable Nitrogen Isotope Analysis, BSIA-$\delta^{15}N$

The powder samples (Control and MQ washed: approx. 3.8 mg; H_2O_2 and NaOCl-treated: approx. 17 mg) and HCl-treated samples were weighted into tin capsules for nano-elemental analyzer - isotope ratio mass spectrometry (nano-EA-IRMS). These samples for BSIA-$\delta^{15}N$ were measured using a Thermo Scientific MAT 253 continuous-flow IRMS coupled to a Thermo Scientific Flash EA 2000 with a small-volume setup (see more instrumental details in Schöne & Huang, 2021) at the Institute of Geosciences, University of Mainz, Germany.

The m/z 28 signal intensities were at least 5 times higher than the background signals (Data Set S1). A two-point correction method was applied using USGS40 ($\delta^{15}N = -4.52‰$) and USGS41a ($\delta^{15}N = 47.55‰$), with m/z 28 signal intensities in the range of the measured samples. Calibration batches of two standards were placed at the beginning and at the end of each measuring sequence, and were also inserted after each 21st to 24th sample. Triplicate USGS43 ($\delta^{15}N = 8.44‰$; N = 27) samples were blindly measured along with the samples as quality control standards, generating an accuracy of $0.11 \pm 0.06‰$ and a precision of $0.08 \pm 0.08‰$. Due to the limited number of shell powders, a triplicate run within each sub-aliquot sample was not always possible. Given that the average value was calculated from multiple measurements of the same sample, we consider the variance of sub-aliquots by propagating the respective error following Schöne and Huang (2021). The nitrogen concentration was computed based on various amounts of L-glutamic acid that was also processed in the IRMS. The shell nitrogen content was calculated by scaling the measured nitrogen content (organic fraction of the samples) up to the mass of shell powder that was originally analyzed.

2.4. Pretreatment for and Measurement of AA Compositions

The sub-aliquots of powders (Control and MQ washed: 30–50 mg; H_2O_2 and NaOCl treated: 70–100 mg) or HCl-treated samples from each treatment group were transferred into 40 mL glass tubes equipped with a polypropylene cap and unbonded septa (Thermo Fisher, USA). 1 mL of HCl (1 N) was added to the tubes with gentle shaking to gradually dissolve the calcium carbonate, which was repeated until the bubbling completely ceased. AAs were extracted by hydrolysis in HCl with a final concentration of 6 N at 110°C for 24 hr. The samples were dried at 50°C in a vacuum concentrator (SPD140DDA, Thermo Fisher, USA). The dried hydrolysates then went through a demineralization procedure to remove Ca^{2+} and other interfering matrices using a cation exchange resin (Dowex AG 50W-X8 resin), following the procedure of Takano et al. (2010) with slight modifications (Huang, Wu, & Schöne, 2023). Briefly, a 5 g Dowex AG 50W-X8 hydrogen form resin (200–400 mesh; Acros Organics, Thermo Fisher Scientific, Geel, Belgium) was packed in a glass pipette column and plugged with pre-combusted glass wool. The resin was conditioned with 1 N HCl (×3 volumes of resin, i.e., three bed-volumes) and rinsed with four bed-volumes of MQ water. Hydrolyzed samples were redissolved in 3 mL of 0.1 N HCl and then loaded into the glass pipette column, followed by flushing with three bed-volume of MQ water. The AA fraction was eluted and collected by rinsing with three bed-volumes of 10 vol% NH_3 in H_2O, dried using a vacuum concentrator and stored in 1 mL of 0.1 N HCl until measurement.

The samples were filtered through 0.22 μm polytetrafluoroethylene membrane filters, and their AA abundances were quantified by a high-performance liquid chromatograph (HPLC; Agilent 1260 infinity II) equipped with a guard column (5 mm × 4.6 mm i.d. × 2.7 μm particle size, Agilent Technologies, USA) and an Agilent AdvanceBio AAA column (100 mm × 4.6 mm i.d. × 2.7 μm particle size, Agilent Technologies, USA). An online pre-column derivatization with 9-fluorenylmethyloxycarbonyl (FMOC) and o-phthalaldehyde (OPA) was conducted in the HPLC system using a multi-injection method. Separation of AAs was performed using two mobile phases, that is, mobile phase A (10 mM Na_2HPO_4 and 10 mM $Na_2B_4O_7$ decahydrate, pH = 8.2) and mobile phase B (acetonitrile, methanol and H_2O, 45:45:10, v:v:v), at a flow rate of 1.5 mL min^{-1} following a gradient program: 0–0.35 min, 2% B, 0.35–13.4 min, 57% B, 13.4–13.5 min, 100% B, 13.5–15.7 min, 100% B, 15.7–15.8 min, 2% B, and 15.8–18.0 min, 2% B. The diode array detector was set at wavelengths of 338 and 262 nm to detect OPA and FMOC-derivatized AAs, respectively. The individual AAs were identified by comparing the retention times with that of an AA standard mix (1 nmol μL^{-1} in 0.1 N HCl; Agilent Technologies, USA) and quantified by using the calibration equations generated by the standard mix for each AA. Note that hydrolysis during pretreatment turned glutamin (Gln) to glutamic acid (Glu) and asparagine (Asn) to aspartic acid (Asp), resulting in the measurement of Gln + Glu and Asn + Asp, which are noted as Glx and Asx in this study. The above protocol recovered 15 AAs: Glx, Asx, alanine (Ala), leucine (Leu), isoleucine (Ile), proline (Pro), valine (Val), glycine (Gly), serine (Ser), lysin (Lys), phenylalanine (Phe), tyrosine (Tyr), histidine (His), arginine (Arg), and threonine (Thr). After measuring the AA concentrations, the results were converted to molar percentages, that is, the AA relative abundances.

2.5. Nitrogen Isotope Analysis of AAs, CSIA-$\delta^{15}N_{AA}$

To determine the nitrogen isotope composition of individual AA ($\delta^{15}N_{AA}$) of shell organics, additional aliquots (three sub-aliquots each) were taken from two of the studied specimens (Shell B and Shell C). Shell A was not sampled here because the remaining sample amount was not enough for CSIA-$\delta^{15}N_{AA}$. All samples were

hydrolyzed, demineralized and derivatized using methods described in Huang, Wu, and Schöne (2023), prior to CSIA-$\delta^{15}N_{AA}$. Briefly, this entailed the hydrolysis of individual aliquots of dried shell powder undergone the experimental treatments (approximately 100–120 mg for Control, 500–700 mg for H_2O_2 and NaOCl groups) with norvaline as an internal standard (50 μg mL^{-1}), followed by demineralization and isolation of the AA fraction by means of ion exchange chromatography described in Section 2.4. The purified AAs were then derivatized to *N*-acetyl-*i*-propyl (NAIP) esters after Styring et al. (2012) with slight modifications (for details, see Huang, Wu, & Schöne, 2023). The derivatives were stored in a GC vial with an insert in 100 μL ethyl acetate and stored at −20°C prior to analysis. $\delta^{15}N_{AA}$ values were determined by gas chromatography-combustion-isotope ratio mass spectrometry (GC-C-IRMS) using a Thermo Trace GC Ultragas chromatograph, fitted with an Agilent DB-35 GC column (60 m × 0.32 mm i.d. × 0.5 μm film thickness, Agilent, USA), coupled to a Delta V plus IRMS via a GC IsoLink II combustion interface. The GC oven was set as follows: 40°C (hold 5 min) to 120°C at 15°C min^{-1}, to 180°C at 3°C min^{-1}, to 210°C at 1.5°C min^{-1}, and to 280°C at 3.5°C min^{-1} (hold 8 min). Pulses of reference gas (N_2) were introduced into the IRMS during the analysis giving rise to peaks with known $\delta^{15}N$ values (^{15}N:^{14}N ratio relative to air N_2) and were used to calculate the analyte peaks in each chromatogram. Identification of the derivatized AAs was conducted by matching the peak retention times with those from a mixed AA standard (derivatized). Samples were injected in triplicate and bracketed by standards and blanks. Sample $\delta^{15}N$ values were corrected in four steps described by Huang, Wu, and Schöne (2023) based on (a) the effect of low $\delta^{15}N_{AA}$ signal areas, (b) AA-specific $\delta^{15}N_{AA}$ drift during analytical sequences, (c) the use of internal standard material, and (d) scale-normalization. The long-term precision computed from the mixed AA standard data that were processed along with the samples was better than 1‰, except for Ala, Leu and Val (1–1.5‰). All samples were treated, derivatized and measured at the Institute of Geosciences, University of Mainz, Germany.

2.6. Mass Balance Calculation

To address the potential offset in bulk $\delta^{15}N$ values between intra-OM and raw-OM pools, it was considered that both pools contained nitrogen derived from the total hydrolyzable amino acids (THAA) and the rest of OM (rest-OM). The contributions from the two fractions (THAA and rest-OM) to bulk $\delta^{15}N$ values were further calculated. For the fraction of THAA, $\delta^{15}N_{AA}$ values were firstly weighted by their molar percentage of each AA (mol $\%_{AA}$):

$$\delta^{15}N_{\text{weighted AA}} = \delta^{15}N_{AA} \times \text{mol}\,\%_{AA}. \quad (1)$$

The estimated $\delta^{15}N$ values of THAA ($\delta^{15}N_{THAA}$) was calculated using a mass balance equation that summed up all $\delta^{15}N_{\text{weighted AA}}$ values in Equation 1, yielding

$$\delta^{15}N_{THAA} = \Sigma(\delta^{15}N_{AA} \times \text{mol}\,\%_{AA}). \quad (2)$$

The contribution from the THAA fraction ($\delta^{15}N_{\text{weighted THAA}}$) to bulk $\delta^{15}N$ values was calculated using $\delta^{15}N_{THAA}$, weighted by their relative nitrogen content:

$$\delta^{15}N_{\text{weighted THAA}} = \delta^{15}N_{THAA} \times f_{THAA}, \quad (3)$$

where f_{THAA} was the nitrogen content of THAA (N $\%_{THAA}$) relative to the bulk nitrogen content (N $\%_{bulk}$) of the studied organic pool. N $\%_{THAA}$ was computed from the measured AA concentrations via HPLC, while N $\%_{bulk}$ was measured via EA-IRMS. In turn, the contributions from the rest-OM to bulk $\delta^{15}N$ values ($\delta^{15}N_{\text{rest-OM}} \times f_{\text{rest-OM}}$, or $\delta^{15}N_{\text{weighted rest-OM}}$) and their nitrogen isotope compositions ($\delta^{15}N_{\text{rest-OM}}$) can be further computed by a combination of Equations 4 and 5:

$$\delta^{15}N_{\text{rest-OM}} \times f_{\text{rest-OM}} = \delta^{15}N_{\text{bulk}} - \delta^{15}N_{THAA} \times f_{THAA}, \quad (4)$$

$$f_{\text{rest-OM}} = \frac{\text{N}\,\%_{\text{bulk}} - \text{N}\,\%_{THAA}}{\text{N}\,\%_{\text{bulk}}}, \quad (5)$$

where $f_{\text{rest-OM}}$ stands for the nitrogen content of rest-OM in the studied organic pool relative to the bulk nitrogen content.

2.7. Statistics

The effect of cleaning treatments on bulk $\delta^{15}N$ values was tested by mixed models considering the three individual shells as a random factor. Statistical differences in AA composition among treatments were tested by

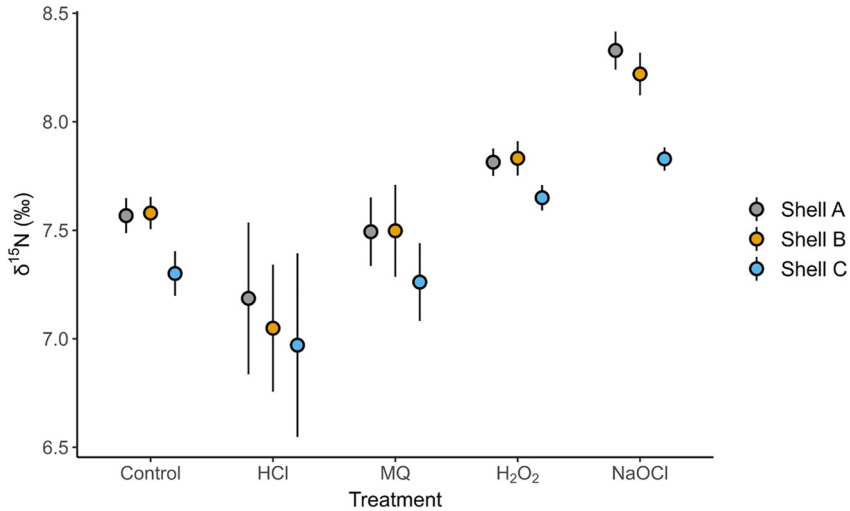

Figure 2. Pretreatment effects on $\delta^{15}N$ values (mean ± 1σ) of three *Arctica islandica* shells. The control group stands for "no treatment." Shell powders were immersed in different solvents including acid (HCl), MilliQ (MQ) water and two oxidation reagents (H_2O_2, NaOCl). Error bars = 1σ propagated error estimated on the basis of the standard deviation of three sub-aliquots (i.e., replicates for each treatment group) and repeated measurements within one sub-aliquot.

permutational multivariate analysis (PERMANOVA), considering the treatment group as a fixed factor and the individual shell as a random factor. PERMANOVA was run on a resemblance matrix based on Euclidean distance measures and with 999 permutations (Anderson & Braak, 2003). The relative abundance data of AAs from three specimens were then pooled for the analyses because the patterns were nearly invariant between specimens (Data Set S1). The groupings in terms of AA composition among treatments were visualized by principal components analysis (PCA) based on the Euclidean distance matrix of relative AA abundance profiles. AAs were further categorized as trophic (Ala, Asx, Glx, Ile, Leu, Pro, and Val), source (Lys, Tyr, Phe, Met, Gly, and Ser) and metabolic (Thr) groups according to previous studies (Germain et al., 2013; Popp et al., 2007) and statistically significant differences among treatment groups were tested by the analysis of variance (ANOVA) following Tukey's HSD test. The effect of different oxidation reagents on $\delta^{15}N_{AA}$ values was evaluated using non-parametric Kruskal-Wallis tests due to the violation of data normality (Shapiro's test) or homoscedasticity (Levene's test). These statistical analyses were conducted using the R software (R Core Team, 2021) with packages lme4 (Bates et al., 2015) and lmerTest (Kuznetsova et al., 2017) for mixed models, Factoextra (Kassambara & Mundt, 2017) for PCA, vegan (Oksanen et al., 2018) and pairwiseAdonis R (Martinez Arbizu, 2019) for PERMANOVAs, and car (Fox & Weisberg, 2019) for ANOVA and Kruskal-Wallis tests.

3. Results

3.1. Bulk $\delta^{15}N$ Values and Nitrogen Contents After Different Treatments

There was a significant effect of cleaning techniques on BSIA-$\delta^{15}N$ values of the treated shell powders ($F_{4, 51}$ = 58.39, P < 0.05). The bulk $\delta^{15}N$ values of the shell organics differed among treatments, except for the comparison between the Control group and powders treated with MQ water (P = 0.87). The shell organics extracted by HCl (i.e., the acid-insoluble fraction) showed the lowest $\delta^{15}N$ values and were, on average, 0.4‰ lower than the Control group (P < 0.05), while $\delta^{15}N$ values of "intra-OM" extracted by H_2O_2 and NaOCl were higher than those of the other groups (P < 0.05; Figure 2). Specifically, the NaOCl group was most enriched in ^{15}N and, on average, 0.6 and 0.4‰ higher than those of the Control and H_2O_2 groups, respectively (P < 0.05). In addition, a significant $\delta^{15}N$ difference was observed between individual specimens (P < 0.05), with Shell C showing the lowest values compared with the other two specimens (Figure 2). This difference was generally found in all groups, but the large variation between replicates within the HCl treatment diminished this difference (Figure 2).

The nitrogen content of the original shell powder (Control group) equaled 46.5 ± 0.4 to 50.7 ± 0.2 nmol mg^{-1} (Figure S1 in Supporting Information S1). When scaling up the data from the mass of shell OM to the original

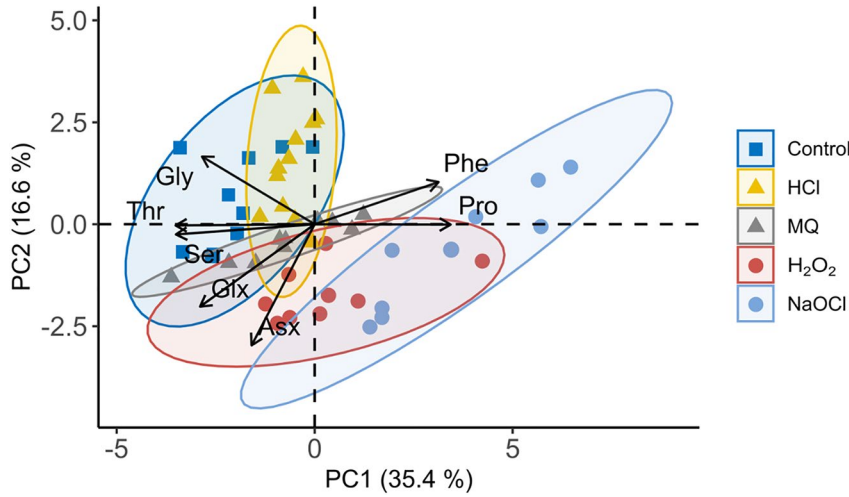

Figure 3. Multivariate separation of measured amino acid (AA) composition of shell organic matrices of *Arctica islandica* extracted with different solvents, visualized using a principal component analysis (PCA) with 95% ellipses for each group. The treatment groups included the control group (no treatment) and shell powders treated with acid (HCl), MilliQ (MQ) water and oxidation reagents (H_2O_2, NaOCl). Arrows show the direction and magnitude of the eigenvectors of the AA correlating >70% with the first two PC axes.

mass of shell powders prior to any treatment, the powders that underwent the HCl treatment had the lowest amount of nitrogen ranging from 4.1 ± 2.4 to 10.6 ± 2.4 nmol mg^{-1} (Figure S1 in Supporting Information S1) and the least nitrogen recovery (9%–21%) of all treatments. On the contrary, powders washed exclusively with MQ water yielded 91%–94% of nitrogen with a nitrogen content of 42.4 ± 2.4 to 45.9 ± 1.0 nmol mg^{-1} (Figure S1 in Supporting Information S1). For the extracted "intra-OM," the nitrogen content of the NaOCl-treated samples (10.2 ± 0.6 to 10.6 ± 0.4 nmol mg^{-1}) was three times lower than those treated with H_2O_2 (Figure S1 in Supporting Information S1), recovering only 21%–23% of nitrogen from the original shell powder.

3.2. AA Molar Abundance and Composition Between Treatments

Among the 15 AAs that were confidently measured, Asx, Gly, Glx, Pro, and Ala were the most abundant in all shell organic phases, each of which constituted more than 9 wt% of the total AAs (Figure S3 and Table S1 in Supporting Information S1). The AA composition based on Mol% showed differences between treatments, which were revealed by PCA (Figure 3) and confirmed by PERMANOVA ($F_{4, 40} = 7.831$, $P < 0.05$). The AA composition of the NaOCl group was distinct from the Control, MQ and HCl groups based on non-overlapping 95% confidence ellipses (Figure 3) and significant differences detected by PERMANOVA tests (pairwise $P < 0.05$). Significantly higher percentages of Pro, Phe and Arg as well as lower percentages of Gly, Ser, and Thr were detected in the NaOCl group (Figure S3 and Table S1 in Supporting Information S1), consistent with the identified AAs that contributed substantially to the separation by PCA loadings (Figure 3). The AA composition between the H_2O_2 group and other groups was also visually distinct with slight overlaps of the 95% confidence ellipses (Figure 3) where significant differences in AA composition were detected (PERMANOVA test: pairwise $P < 0.05$). Most of the AA mol % in the H_2O_2 group ranged between values of the Control and NaOCl groups (Figure S3 and Table S1 in Supporting Information S1). Samples of the Control group showed extensive overlap in AA composition with those of the MQ group (Figure 3), without significant differences in AA composition (PERMANOVA pairwise $P < 0.05$) and AA mol %. Despite a large overlap, the AA composition of the HCl group differed significantly from the Control group (PERMANOVA pairwise $P < 0.05$; Figure 3). The most noticeable AA mol% difference compared to the Control group was found in Arg, which was 3.5 times higher in the HCl group (Figure S3 and Table S1 in Supporting Information S1). Furthermore, after pooling AAs into trophic, source and metabolic categories, the HCl group showed a larger proportion of source AAs than other treatments, while higher proportions in trophic AAs were observed in the H_2O_2 and NaOCl groups (Figure S4 in Supporting Information S1). Metabolic AAs were the rarest in the NaOCl group (Figure S4 in Supporting Information S1).

Consistent with the observations in bulk nitrogen content, the total AA number of shell powders treated with HCl was low (only 13–27 wt% of AAs remained in the extracted organics), while the majority of AAs (85–94 wt%) were still present after rinsing with MQ water (Figure S2 in Supporting Information S1). The two treatments used to isolate intra-OM produced significantly different total AA amounts (Figure S2 in Supporting Information S1). NaOCl-extracted intra-OM contained particularly small amounts of total AA (19–24 wt% of the original shell AA amount) compared to samples treated with H_2O_2 (63–80 wt%).

3.3. AA Nitrogen Isotope Values and Offsets

A consistent $\delta^{15}N_{AA}$ pattern was observed in all measured shell samples, that is, trophic AAs showed higher $\delta^{15}N$ values than source AAs, and metabolic AAs were most depleted in ^{15}N (Figure S5 in Supporting Information S1). The $\delta^{15}N_{AA}$ differences between Shell B and Shell C were significant, which is consistent with the observation of their bulk nitrogen isotope compositions, and such differences were greater than those caused by sample treatments. Therefore, CSIA-$\delta^{15}N_{AA}$ data for the two shells were presented separately. Samples treated with H_2O_2 or NaOCl (used to oxidate inter-OM and isolate intra-OM) only showed significantly different $\delta^{15}N$ values in a few AAs, that is, Glx, Asx, and Gly in Shell C (statistics in Data Set S1), but the offset $\delta^{15}N_{H2O2\text{-}NaOCl}$ values were relatively small (−1.3‰, −1.6‰, and −1.2‰, respectively).

Compared to the nitrogen isotope compositions of AAs of the Control group, most AAs showed similar $\delta^{15}N$ values in Control and treatment groups and located close to the 1:1 line (Figure S6 in Supporting Information S1, Figure 4). The $\delta^{15}N$ offset values (H_2O_2 vs. Control or NaOCl vs. Control) were small and typically remained within the range of the analytical errors, except that Glx, Asx, and Ala sometimes showed large offsets which were not always consistent between the two studied shells (Figure 4, Figure S6 in Supporting Information S1). For further comparison, the organics measured in the NaOCl group are henceforth referred to as intra-OM because NaOCl protocol appears to be capable of extracting the pristine intra-OM (see Section 4.2), while organics in the Control group are referred to as raw-OM. It is important to note that the nitrogen isotope offset of Glx between the Control group (raw-OM) and the NaOCl treatment (intra-OM) was relatively large, approximately three times the long-term analytical precision of $\delta^{15}N_{Glx}$, and such an offset was consistently observed in the two tested shells.

3.4. Mass Balance $\delta^{15}N$ of AA-Derived and Other Nitrogen

$\delta^{15}N_{THAA}$ and bulk $\delta^{15}N$ differed by less than 1‰ (Table 1). Intra-OM contained slightly larger proportions of total AA-derived nitrogen relative to bulk nitrogen (f_{THAA} on average 59 wt%) than that of the raw-OM pool (f_{THAA}, on average, 55 wt%). Considering the relative nitrogen amounts, the fraction of AA-derived nitrogen ($\delta^{15}N_{weighted\ THAA} = \delta^{15}N_{THAA} \times f_{THAA}$) equaled approx. 65 and 57 wt% of the bulk $\delta^{15}N$ values in the intra-OM and raw-OM pools, respectively. The total AA contribution to bulk $\delta^{15}N$ values ($\delta^{15}N_{weighted\ THAA}$) also reflected nitrogen isotope differences between intra-OM and raw-OM in a similar manner as observed by the bulk analysis (see the intra-OM to raw-OM offsets in Table 2), although this total AA-derived fraction showed a slightly more pronounced offset (measured bulk approach: 0.6 and 0.5‰ in Shell B and Shell C; calculated THAA fraction: 1.0 and 0.8‰ in Shell B and Shell C). To compute the balance, the rest-OM fraction contributed negatively (−0.4‰ and −0.3‰ in Shell B and Shell C; Table 2) to the observed positive offset values of bulk $\delta^{15}N$ values because bulk $\delta^{15}N$ values represented the sum of contributions from THAA and rest-OM. Accounting for the relative abundance, Pro showed markedly higher $\delta^{15}N_{weighted\ AA}$ values in the intra-OM than the raw-OM (difference of approx. 1.0‰), while this difference did not exceed 0.3‰ for all other AAs (Table 2).

4. Discussion

As demonstrated, firstly, a very minor nitrogen isotope fractionation occurred after acid washing, one of the most common pretreatments to obtain the shell organics for BSIA-$\delta^{15}N$. However, this solvent generated variability of $\delta^{15}N$ values within replicates. Secondly, the two studied oxidation reagents (NaOCl and H_2O_2) used to extract the intra-crystalline phase of shell organics showed differences in both BSIA- and CSIA-$\delta^{15}N_{AA}$ values. Furthermore, the isotope offsets (both bulk and AA-specific) between intra-OM and raw-OM pools of the studied bivalve shells were assessed. Both the AA composition and $\delta^{15}N_{AA}$ values varied between shell OM pools and together explained the observed offsets in bulk $\delta^{15}N$ values between intra-OM and raw-OM. These results are of critical relevance (a) to determine the nitrogen isotope compositions of raw-OM and intra-OM of bivalve shells

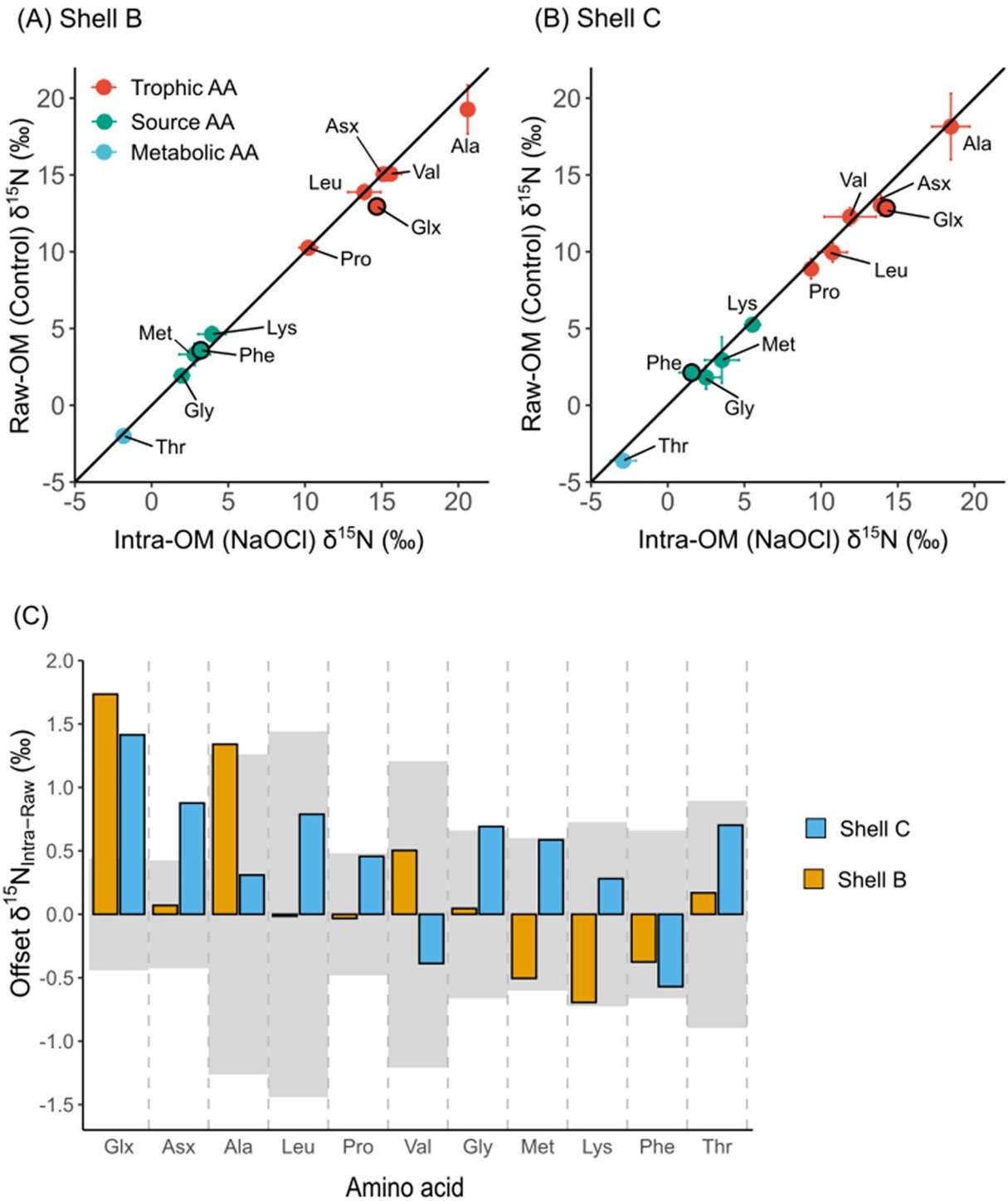

Figure 4. Comparison of individual amino acid (AA) $\delta^{15}N$ values (mean ± 1σ) of the intra-crystalline organic fraction (intra-OM) isolated with NaOCl and raw organics (raw-OM; Control group) in studied *Arctica islandica* specimens. (a) Shell B and (b) Shell C and their average nitrogen isotope offsets (c). In (a) and (b), the solid line represents a 1:1 correlation (line of unity) between $\delta^{15}N$ values in intra-OM and raw-OM. Black lines around circles emphasize phenylalanine (Phe) and glutamic acid (Glx), which are commonly used to calculate the trophic position of consumers. The gray areas in (c) represent the long-term precision (1σ) computed from AA standards measured along with the samples.

Geochemistry, Geophysics, Geosystems

10.1029/2023GC011147

Table 1

Molar Percentage (Mol %) of Amino Acids (AAs), $\delta^{15}N$ Values of AAs ($\delta^{15}N_{AA}$) and Calculated $\delta^{15}N$ Values of Total Hydrolyzable Amino Acids (THAA) ($\delta^{15}N_{THAA}$) and the Rest of Organic Matter ($\delta^{15}N_{rest\text{-}OM}$) and Their Contributions to Bulk $\delta^{15}N$ Values ($\delta^{15}N_{weighted\ THAA}$ and $\delta^{15}N_{weighted\ Rest\text{-}OM}$), Respectively Considering Their Relative Nitrogen Content to the Bulk Nitrogen Content ($\delta^{15}N_{THAA} \times f_{THAA}$ or $\delta^{15}N_{rest\text{-}OM} \times F_{rest\text{-}OM}$)

	Mol (%)				$\delta^{15}N_{AA}$ (‰)				$\delta^{15}N_{weighted\ AA}$ (‰) = mol (%) × $\delta^{15}N_{AA}$ (‰)			
AA	Shell B		Shell C		Shell B		Shell C		Shell B		Shell C	
(A) Intra-OM	Mean	1σ	Mean	1σ	Mean	1σ	Mean	1σ	Mean	1σ	Mean	1σ
Ala	9.1	0.3	9.7	1.0	20.6	1.5	18.5	1.2	1.9	0.2	1.8	0.2
Arg	3.2	0.0	3.2	1.6	NA		NA					
Asx	12.2	0.2	13.7	0.9	15.1	0.4	13.9	0.3	1.9	0.1	1.9	0.1
Glx	9.2	0.1	10.6	0.6	14.7	0.2	14.3	0.3	1.4	0.0	1.5	0.1
Gly	8.1	0.4	10.0	0.8	2.0	0.5	2.5	0.9	0.2	0.0	0.2	0.1
His	0.8	1.4	1.1	0.0	NA		NA					
Ile	2.1	0.7	1.9	0.1	NA		NA					
Leu	2.6	0.1	3.0	0.1	13.9	1.1	10.7	1.0	0.4	0.0	0.3	0.0
Lys	4.0	0.1	4.1	0.1	3.9	0.9	5.5	0.5	0.2	0.0	0.2	0.0
Met	NA		NA		2.8	1.0	3.5	1.1				
Phe	6.9	1.3	3.5	0.3	3.2	0.3	1.6	0.8	0.2	0.0	0.1	0.0
Pro	23.4	1.6	20.9	5.7	10.2	0.6	9.3	0.3	2.4	0.2	2.0	0.5
Ser	5.3	0.1	6.0	0.4	NA		NA					
Thr	5.0	0.1	5.0	0.3	−1.8	0.2	−2.9	0.9	−0.1	0.0	−0.1	0.0
Tyr	2.6	0.5	2.8	0.0	NA		NA					
Val	5.4	0.2	4.4	0.2	15.6	0.7	11.9	1.7	0.8	0.0	0.5	0.1
Calculated $\delta^{15}N_{THAA}$ (‰)									9.1	0.3	8.4	0.6
f_{THAA}	57.7	3.9	61.1	2.0								
Calculated $\delta^{15}N_{weighted\ THAA}$ (‰)									5.2	0.4	5.1	0.4
Measured bulk $\delta^{15}N$ (‰)									8.2	0.2	7.8	0.2
Calculated $\delta^{15}N_{rest\text{-}OM}$ (‰)									7.0	0.7	6.9	0.6
Calculated $\delta^{15}N_{weighted\ rest\text{-}OM}$ (‰)									3.0	0.4	2.7	0.3
(B) Raw-OM	Mean	1σ	Mean	1σ	Mean	1σ	Mean	1σ	Mean	1σ	Mean	1σ
Ala	10.5	0.3	10.0	0.7	19.3	1.6	18.2	2.2	2.0	0.2	1.8	0.3
Arg	1.0	0.5	1.5	0.3	NA		NA					
Asx	14.0	2.9	15.0	1.7	15.0	0.3	13.0	0.7	2.1	0.4	2.0	0.2
Glx	12.5	0.4	11.6	0.9	12.9	0.2	12.8	0.2	1.6	0.1	1.5	0.1
Gly	14.7	0.8	12.5	1.0	1.9	0.3	1.8	0.8	0.3	0.0	0.2	0.1
His	0.9	0.4	1.0	0.0	NA		NA					
Ile	2.4	0.6	2.0	0.1	NA		NA					
Leu	3.4	0.2	3.5	0.2	13.9	0.5	10.0	0.6	0.5	0.0	0.4	0.0

Table 1
Continued

(B) Raw-OM	Mean	1σ	Mean	1σ	Mean	1σ	Mean	1σ	Mean	1σ	Mean	1σ
Lys	4.3	1.9	5.8	1.4	4.6	0.5	5.2	0.3	0.2	0.1	0.3	0.1
Met	NA		NA		3.3	0.7	2.9	1.5				
Phe	2.3	0.2	2.6	0.4	3.6	0.5	2.1	0.5	0.1	0.0	0.1	0.0
Pro	8.5	2.4	10.2	2.9	10.3	0.3	8.9	0.7	0.9	0.2	0.9	0.3
Ser	8.4	0.6	8.0	0.7	NA		NA					
Thr	9.1	0.2	8.5	0.6	−2.0	0.4	−3.6	0.3	−0.2	0.0	−0.3	0.0
Tyr	3.2	0.3	3.0	0.2	NA		NA					
Val	4.8	0.9	4.6	0.8	15.1	0.4	12.3	0.6	0.7	0.1	0.6	0.1
Calculated $\delta^{15}N_{THAA}$ (‰)									8.2	0.6	7.4	0.5
f_{THAA}	51.5	1.1	58.2	7.6								
Calculated $\delta^{15}N_{weighted\ THAA}$ (‰)									4.2	0.3	4.3	0.6
Measured bulk $\delta^{15}N$ (‰)									7.6	0.2	7.3	0.2
Calculated $\delta^{15}N_{rest\text{-}OM}$ (‰)									6.9	0.6	7.2	1.4
Calculated $\delta^{15}N_{weighted\ rest\text{-}OM}$ (‰)									3.4	0.3	3.0	0.7

Note. "NA" denotes the undetectable AAs.

and (b) to unravel the mechanisms causing isotope offsets between different OM pools. This information is crucial for employing shell organic phases to infer details on the nitrogen biogeochemistry of aquatic environments.

4.1. Acid Washing Affects the Nitrogen Isotope Composition of Shell Organics

In this study, acid washing caused a very small but significant depletion in ^{15}N (within 0.5‰) of shell samples. While other studies on bivalve shells rather found the acid effect insignificant (Carmichael et al., 2008; Darrow et al., 2017), the result herein is in agreement with a study that showed a small deviation existed in bulk $\delta^{15}N$ values of acid-extracted shell organics (+0.7‰; Pape et al., 2018). As discussed in more detail below, the possible mechanism causing the observed minor fractionation is the removal of the soluble organic matrix during decantation. It was shown that washing with MQ water alone did not result in any statistically noticeable changes in the bulk nitrogen isotope composition (Figure 2). The relative abundances and compositions of AAs remained similar between the control and MQ washing groups (Figure 3 and Figure S3 in Supporting Information S1), suggesting that the AA-derived (mostly protein-derived) organics were also not altered after MQ washing. After all, the interstitial soluble fraction of shell biomolecules represents only a small amount (Almeida et al., 2000; Marin et al., 2007; Pereira-Mouriès et al., 2002) and typically comprises less than 10 wt% nitrogen of the raw-OM (Figure S1 in Supporting Information S1). In comparison, the HCl-treated remainders exhibited relatively low recovery rates in bulk nitrogen content (9–21 wt%; Figure S1 in Supporting Information S1) and total AA concentration (13–23 wt%; Figure S2 in Supporting Information S1), suggesting that more than 79 wt% bulk nitrogen and more than 77 wt% AAs were lost during acid washing. This is likely because the soluble organic moieties which were cast away during acid washing contained a completely different organic composition than organics soluble in MQ water. Firstly, the acid washing dissolved calcium carbonate and released the intra-crystalline organic matrix trapped within the biominerals. This caused a severe loss of soluble materials. Secondly, the acid treatment altered the pH conditions, that is, the pH decreased to <1 during the HCl extraction, which changed the solubility of proteins (Riès-kautt & Ducruix, 1997; Tseng et al., 2009). Compared with the raw-OM, the HCl extracts showed a different AA composition, indicating the lost nitrogenous materials consisted of at least a different set of proteins that were possibly rich in Ser and Glx and low in Arg (Figure 3 and Figure S3 in Supporting Information S1). The significant differences in the proportions of AA groups categorized by nitrogen isotopic fractionation, that is, a lower proportion of trophic AAs with elevated ^{15}N content in combination with a higher proportion of source AAs which barely fractionate during the trophic transfer (Chikaraishi et al., 2009), suggest that this fraction of soluble proteins has higher $\delta^{15}N$ values. In addition, up to 55 wt% of the nitrogen loss during acid treatment can largely be attributed to nitrogen deriving from protein-AAs (Data Set S1). This observation suggests that, apart from proteins, the lost soluble fraction during acid extraction also comprised other nitrogen-bearing compounds, for example, glycosaminoglycans, amino sugars, or nucleic acids/bases (Agbaje et al., 2019; Ferreira et al., 2020; Marxen & Becker, 1997). The loss of this portion during the decantation could also have contributed to the deviation of the BSIA-$\delta^{15}N$ values of shell organics. Future studies should therefore target non-AA

Table 2
Differences (or Offset Values) Between Intra-Crystalline and Raw Shell Organic Pools (Intra-OM and Raw-OM) in Molar Percentage (Mol %) of Amino Acid (AA), Individual AA $\delta^{15}N$ Values ($\delta^{15}N_{AA}$) and Their Corresponding $\delta^{15}N_{weighted\ AA}$ Values (Weighted by Mol %)

	Offset values between intra-OM and raw-OM					
	Mol %		$\delta^{15}N_{AA}$ (‰)		$\delta^{15}N_{weighted\ AA}$ (‰) = mol (%) × $\delta^{15}N_{AA}$ (‰)	
AA	Shell B	Shell C	Shell B	Shell C	Shell B	Shell C
Ala	−1.4	−0.3	1.3	0.3	−0.1	0.0
Arg	2.2	1.6	NA	NA		
Asx	−1.7	−1.3	0.1	0.9	−0.2	−0.1
Glx	−3.3	−1.0	1.7	1.4	−0.3	0.0
Gly	−6.7	−2.5	0.0	0.7	−0.1	0.0
His	−0.1	0.1	NA	NA		
Ile	−0.4	−0.1	NA	NA		
Leu	−0.8	−0.5	0.0	0.8	−0.1	0.0
Lys	−0.3	−1.7	−0.7	0.3	0.0	−0.1
Met	NA	NA	−0.5	0.6		
Phe	4.5	0.9	−0.4	−0.6	0.1	0.0
Pro	14.9	10.7	0.0	0.5	1.5	1.0
Ser	−3.1	−2.0	NA	NA		
Thr	−4.1	−3.5	0.2	0.7	0.1	0.2
Tyr	−0.6	−0.3	NA	NA		
Val	0.6	−0.2	0.5	−0.4	0.1	0.0
Intra-OM to raw-OM offset of measured bulk $\delta^{15}N$ (‰):					0.6	0.5
Intra-OM to raw-OM offset of $\delta^{15}N_{weighted\ THAA}$ (‰):					1.0	0.8
Intra-OM to raw-OM offset of $\delta^{15}N_{weighted\ rest\text{-}OM}$ (‰):					−0.4	−0.3

Note. This yielded the intra-OM to raw-OM offset values from fractions of the total hydrolyzable amino acids (THAA) and the rest of organic matter (rest-OM) to bulk $\delta^{15}N$ values, noted as $\delta^{15}N_{weighted\ THAA}$ and $\delta^{15}N_{weighted\ rest\text{-}OM}$, that considered their relative nitrogen content to the bulk nitrogen content (see Table 1). "NA" denotes the undetectable AAs.

nitrogen. It has been speculated that isotopic fractionation could occur during the hydrolysis of proteinaceous compounds, for example, by the break-up of the peptide bonds of proteins and subsequent loss in discarded solutions (Brault et al., 2014; Mateo et al., 2008; Schlacher & Connolly, 2014). However, given the preferential hydrolysis of ^{12}C-^{14}N bonds, this process would rather lead to enrichment in ^{15}N in the remaining unhydrolyzed protein (Bada et al., 1989; Silfer et al., 1992), which contradicts the results herein. The same line of reasoning applies to the third possible process that might have affected the nitrogen isotope composition of the extracted shell organics, that is, volatilization of nitrogenous compounds (such as chloramine), which would rather cause enrichment of ^{15}N in the remainders instead of depletion.

The present study also revealed inter-specimen variations in BSIA-$\delta^{15}N$ values of original shell organics (i.e., raw-OM of the Control group), that is, Shell C showed lower $\delta^{15}N$ values than the other two shells. As bivalves mainly filter phytoplankton from the water (Newell, 2004), $\delta^{15}N$ values in primary producers (i.e., nitrogen isotope baseline) that register changes in environmental nitrogen sources influence the $\delta^{15}N$ values in both soft and hard tissues of bivalves (e.g., Graniero et al., 2021; Vokhshoori et al., 2022). Given that we have measured the homogenized whole valve of each specimen, the inter-specimen variation in shell nitrogen isotope compositions could be attributed to differences in the time intervals during which the shells formed. Unfortunately, the ontogenetic ages of the studied specimens have not been determined, but they may be inferred from the size of the shells and previous analyses of specimens from the same study site (Marali et al., 2017). Shell C was slightly larger than Shell A and Shell B, indicating that it was older and lived during somewhat different calendar years and hence recorded another set of dietary and environmental nitrogen information. In addition, it is also possible that the

diet slightly varied within specimens of the same population resulting from microhabitat differences, for example, the "patchiness" of microphytobenthos (Seuront & Spilmont, 2002). However, this inter-specific $\delta^{15}N$ variation was not observed in the HCl group, possibly because of the unavoidable loss of shell powder during the repetitive centrifugation and decantation that introduced errors to the results. This observation indicates that acid washing can introduce variability of the nitrogen isotope data between experimental replicates, which in turn might blur the real differences in real differences in nitrogen isotope compositions between specimens.

4.2. Oxidation Reagents Affect the Nitrogen Isotope Composition of Intra-Crystalline Organics

Given the vigorous oxidation capability, NaOCl is widely used in the protocols to effectively remove weakly bound inter-OM of gastropods (Demarchi et al., 2013; Penkman et al., 2008), corals (Wang et al., 2015), fish otoliths (Lueders-Dumont et al., 2018) and tooth enamel (Martínez-García et al., 2022). This pretreatment step is necessary prior to studying the intra-OM, but less work has been focused on bivalve shells (Penkman et al., 2008; Sykes et al., 1995). Previous studies on shells of several mollusk species showed that the individual AA concentrations sharply decreased with NaOCl oxidation time, suggesting that 48 hr of NaOCl treatment is sufficient for subsequent analysis of intra-OM (Demarchi et al., 2013, 2015; Ortiz et al., 2015; Penkman et al., 2008). The grain size of the samples can potentially also affect the NaOCl oxidation efficiency, given that the oxidation reagent may have difficulties in reaching individual biomineral units. For *Patella vulgata*, particle sizes of 500–1,000 μm were small enough to recover the amount of intra-crystalline AA after 48 hr of bleaching, but larger variability of the recovery rate was observed compared to the smaller grain sizes (Demarchi et al., 2013). Smaller grain sizes were less variable in $\delta^{15}N$ values due to a higher level of homogeneity, although insignificant differences in nitrogen content and BSIA-$\delta^{15}N$ data of otolith powder were shown between three grain sizes (>425, 50–425, and 38–150 μm) (Lueders-Dumont et al., 2018). As the predominant portion (>90%) of the shell powder in the present study remained below a grainsize of 500 μm, most of inter-OM should have been efficiently eliminated. Based on the outlined arguments, that is, effective oxidation using the reagent, sufficient time of reaction and the optimal grain size of the samples, the NaOCl-treated shell powders in this study likely contained only the OM entrapped within the biominerals, that is, the intra-OM. Moreover, the use of NaOCl results in a "cleaner" chromatogram for CSIA-$\delta^{15}N_{AA}$, which overcomes concerns that the Cl-containing by-products may interfere with the combustion and reduction process during the GC-C-IRMS procedure. However, this protocol requires more thorough rinsing with MQ water to wash NaOCl out. Here, at least 4 times of rinsing was necessary to neutralize the samples.

Furthermore, the nitrogen content and total AA content in H_2O_2-extracted organics were at least three times higher than those in the NaOCl group (Figure S1 in Supporting Information S1), suggesting that the removal of inter-OM via immersion in H_2O_2 for 48 hr is incomplete. This is supported by the AA composition and the BSIA-$\delta^{15}N$ data. Firstly, AA compositions were statistically distinct between "intra-OM" extracted by these two oxidation treatments, with the H_2O_2 extract showing an AA composition that resembled that of raw-OM (Figure 3). Secondly, the bulk $\delta^{15}N$ values of H_2O_2-extracted organics lay between those of the Control and NaOCl groups (Figure 2), suggesting that the isotope signatures of H_2O_2-extracted "intra-OM" came from a portion of the raw-OM, that is, the inter-OM. Furthermore, after the H_2O_2 treatment, a few AAs (Glx, Asx and Gly) differed in CSIA-$\delta^{15}N_{AA}$ from either the NaOCl or Control treatment (Figures S5 and S6 in Supporting Information S1). For these AAs, whenever a significant difference in $\delta^{15}N_{AA}$ values occurred between the H_2O_2 and NaOCl (presumably intra-OM) or Control (raw-OM, or inter- + intra-OM) treatments, the $\delta^{15}N_{AA}$ values of shell powders oxidized with H_2O_2 always agreed with one of the other groups instead of differing from both groups (i.e., $\delta^{15}N_{Glx,\ Asx,\ and\ Gly}$ values in Shell C: H_2O_2 = Control but H_2O_2 < NaOCl and $\delta^{15}N_{Glx}$ values in Shell B: H_2O_2 = NaOCl but H_2O_2 > Control). This indicates that a portion of the inter-OM that carried a different set of isotope signals in AAs (See Section 4.3) sometimes remained in the H_2O_2 extract. Notably, the change of $\delta^{15}N_{AA}$ values is not consistent between the two studied shells (e.g., $\delta^{15}N_{Glx}$ values in Shell B and Shell C showing Control < H_2O_2 = NaOCl and Control = H_2O_2 < NaOCl, respectively), which could be explained by the inter-specimen variations (see last paragraph of Section 4.1). The results are in line with the suggestions of previous studies, according to which H_2O_2 is less effective in oxidizing the inter-OM than NaOCl, especially when $CaCO_3$ is present (Gaffey & Bronnimann, 1993; Marie et al., 2013; Penkman et al., 2008). H_2O_2 can be thermodynamically unstable, resulting in oxygen bubbling out (Pardieck et al., 1992). Given the acidic nature of H_2O_2 (a pH of 4–5 was measured in this study), minor dissolution of $CaCO_3$ could also have contributed to the bubbling. Small bubbles attached to grain surfaces of shell powder (even at constant shaking) largely prevent the oxidation

reagent from accessing the surface of the crystals where the inter-OM is located, which, therefore, influence the BSIA-$\delta^{15}N$ and CSIA- $\delta^{15}N_{AA}$. Although a longer exposure interval in H_2O_2 may help with the dissolution of the bubbles, considering the oxidation efficiency, NaOCl (specifically at least 48 hr exposure; e.g., Penkman et al., 2008) should be used for the extraction of shell intra-OM, especially for BSIA-$\delta^{15}N$ and CSIA- $\delta^{15}N_{AA}$.

4.3. Differences in Bulk $\delta^{15}N$ Values, AA Composition and $\delta^{15}N_{AA}$ Values of Intra-OM and Raw-OM

Given that inter-OM can be efficiently cleaned after NaOCl treatment as discussed above, hereafter the samples treated by NaOCl are considered to be the intra-crystalline OM (intra-OM). The isotopic composition of intra-OM was found to be more enriched in ^{15}N, with an average difference of 0.6‰ compared to raw OM (raw-OM). In contrast, Pape et al. (2018) observed consistently lower $\delta^{15}N$ values in the intra-OM than in raw-OM of *Mytilus edulis*, *Ruditapes decussatus* and *Cerastoderma edule*. The different $\delta^{15}N_{intra\text{-}raw}$ offsets could result from the different nature of shell biomolecules, given that shell ultrastructures vary largely among bivalve species (Carter, 1990; Currey & Taylor, 1974). For instance, distinct prismatic ultrastructures are present in shells of *M. edulis* (Meenakshi et al., 1973), *R. decussatus* (Popov, 1986), and *C. edule* (Carter, 1990; Denis, 1972), but not in *A. islandica* (Ropes et al., 1984). The chemical composition of shell organics plays a significant role in controlling the growth, size, and shape of biominerals (Gilbert et al., 2022; Hovden et al., 2015; Weiner & Addadi, 1997), producing different ultrastructure types and biomineral unit morphologies at the nanometer scale (Li et al., 2015). As such, the chemistry of the intra-OM may widely differ among and within bivale species (Deng et al., 2022; Okumura et al., 2013). Importantly, distinguishable nitrogen isotope compositions were observed between the intra- and raw organic pools of modern shells in the very few existing BSIA-$\delta^{15}N$ studies (Pape et al., 2018; this study). Such observations imply a different nitrogen isotopic signature in the removed inter-OM given that the raw-OM pool comprises both the inter- and intra-OM fractions. One concern is that the inter-OM can be susceptible to diagenesis, potentially changing the pristine nitrogen isotope composition (Meckler et al., 2008; Robinson et al., 2012; Schubert & Calvert, 2001), but diagenesis is less likely to occur in modern materials that have not undergone extreme thermal degradation (Lueders-Dumont et al., 2018; Martínez-García et al., 2022). The reasonable abundance of Gly and the relative concentration of Ser and Ala (indicators of protein degradation in fossil materials; e.g., Bada et al., 1978; Penkman, 2009) in modern *A. islandica* shells (Agbaje et al., 2017; this study) suggest that the organic degradation process, if present, was negligible. Therefore, we consider the inter-OM as endogenous to the studied bivalve shells.

The organic components that comprise intra-OM and inter-OM can be fundamentally different as a result of different forming procedures during biomineralization (Nudelman et al., 2007). Comparison of the chemistry between OM pools provides clues for this complex process. Biomineral composites of *A. islandica* showed higher amounts of inter-OM than intra-OM (at least 3 times higher in terms of the content of total nitrogen and AAs; Table S2 in Supporting Information S1), which is in agreement with the prismatic layers of *Atrina rigida* (Nudelman et al., 2007). However, the proportions of AA-derived nitrogen were slightly higher in the intra-OM than in the raw-OM pool (Table 1), suggesting that other nitrogen-bearing components, such as polysaccharides, should be richer in the inter-OM. For example, chitin is considered the most abundant compound of the inter-crystalline spaces, forming a scaffolding onto which the acidic proteins and in some cases, a hydrophobic silk gel, will attach for nucleation of $CaCO_3$ (Addadi & Weiner, 1985; Addadi et al., 2006; Gotliv et al., 2003). Yet, this hypothesis is challenged by the results from prismatic shell layers of *A. rigida*, revealing that chitin only resides within calcitic prisms as an intra-crystalline fibrous network (Nudelman et al., 2007). On the other hand, a larger fraction of saccharides in combination with the small amount of chitin in the raw-OM pool of *A. islandica* (Agbaje et al., 2018) calls for a more detailed analysis of other glycosylated polymers between shell organic pools in the future. Moreover, as indicated by the proportion of nitrogen originating from AAs (f_{THAA} in Table 1), proteinaceous materials represent an abundant component of shell organic pools (above 50%), consistent with the previous studies (Addadi & Weiner, 1985; Gotliv et al., 2003; Nudelman et al., 2007). Comparison of AA compositions showed that inter-OM and intra-OM differ in AA compositions (Figure 5), suggesting that different protein species may be present in intra-OM. In previous studies, Ala and Gly, comprising the silk-like and/or gel-like proteins for the crystallization framework (Addadi et al., 2006; Bowen & Tang, 1996; Pereira-Mouriès et al., 2002), were found to be much more abundant in the inter-crystalline space of nacroprismatic shells (e.g., Nudelman et al., 2007). In contrast, Asx and Glx were enriched in the intra-crystalline proteins (e.g., Nudelman et al., 2007; Okumura et al., 2013) given that the acidic and negatively charged features of these AAs allow to bind Ca^{2+} during biomineralization (Addadi & Weiner, 1985; Borukhin et al., 2012; Gotliv et al., 2003).

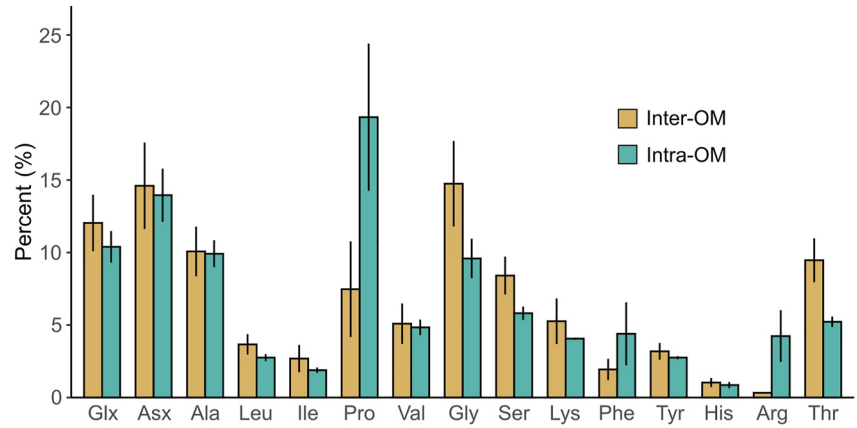

Figure 5. Relative molar percentage (mean ± 1σ) of amino acids (AAs) between inter- and intra-crystalline organic matrices (inter- and intra-OM) of *Arctica islandica* shells. As raw-OM (i.e., the total shell organic matrix) is considered to be the sum of intra-OM and inter-OM, the theoretical concentration of inter-OM was computed by subtracting the measured concentrations of AAs in intra-OM from those in the raw-OM, and the theoretical molar percentages of AAs in inter-OM were further computed. Data were pooled from the three studied shells (Shells A, B, and C) given the insignificant inter-specimen variation.

However, only the relative amount of Gly differed largely between inter- and intra-OM in *A. islandica* shells (Figure 5) and we did not observe any predominance of Asx or Glx in the intra-OM (Figure 5), for example, <14% of Asx in *A. islandica* (this study) but >50% in *A. rigida* (Nudelman et al., 2007). These results suggest a different biomineralization mechanism in *A. islandica*, which predominantly consists of crossed-acicular ultrastructures accompanied by homogeneous, fine complex-crossed lamellar and irregular prismatic/spherulitic ultrastructures depending on the shell layer (Schöne, 2013). Recent findings on the secondary structure of the organic matrix and chemical analyses of bivalve shells revealed a collagen-like material in *A. islandica* shells (Agbaje et al., 2017, 2018). These authors suggested that, instead of using chitin or silk-like proteins to form a β-sheet framework in nacroprismatic shells, a collagen-like proteinaceous material along with polysaccharides including low abundance of chitin can provide scaffolding for the calcium deposition in *A. islandica* shells. Furthermore, we found the hydrophobic and non-polar AA residues, especially Pro and Phe, to be higher in the intra-OM of *A. islandica* shells (Figure 5, Table 2). This agrees with the hypothesis that Ca-binding proteins of *A. islandica* are not limited to acidic proteins, for example, Asx and Glx (Agbaje et al., 2017), but may also relate to the glycosylated proteins that contain large number of hydrophobic AA residues (Fichtner et al., 2017). Another candidate to facilitate the nucleation process would be sulfated macromolecules (Arias & Fernández, 2008; Giuffre et al., 2013; Michenfelder et al., 2003). For instance, sulfated glycoproteins or sugars, as sulfate groups, were found to be enriched at the nucleation sites of *Unio pictorum* (Marie et al., 2007); however, little knowledge of sulfated macromolecules is available for *A. islandica* shells. It should also be noted that the AA composition of inter-OM was computed from the measured AA concentration data of raw-OM (i.e., inter- + intra-OM) and intra-OM, as it is challenging to completely extract and directly measure inter-OM. Although the NaOCl cleaning approach used in this study can extract the pool of intra-OM that is well-protected by the biominerals (Penkman et al., 2008), it remains uncertain and needs to be tested if the cleaning procedure would remove a small fraction of the intra-OM that may bias the computation of inter-OM.

In addition, we contend that the observed $\delta^{15}N$ difference between intra-OM and raw-OM pools is mainly due to the combined influence of relative proportions of individual AA and their $\delta^{15}N$ values. The offset between the intra-OM and raw-OM regarding the AA-derived $\delta^{15}N$ ($\delta^{15}N_{THAA} \times f_{THAA}$) contributed by more than 70 wt% to the observed offset of bulk values (Table 2). This suggests that nitrogen derived from AAs (isotope composition and quantity) largely influenced the small but significant difference in BSIA-$\delta^{15}N$ between the two shell OM pools. It should be mentioned that cysteine, tryptophan and methionine could not be measured with the HPLC method of this study, which may have led to a slight underestimation of AA-derived nitrogen proportions (f_{THAA}). Also, $\delta^{15}N$ values of a few AAs, that is, Arg, His, Ile and Tyr, could not be determined and not included in the mass balance calculation, potentially resulting in an underestimation of the $\delta^{15}N_{THAA}$ values. However, such an underestimation should be negligible as most of these AAs are source AAs with depleted ^{15}N content and their

relative abundances were also low. A close examination of CSIA-$\delta^{15}N_{AA}$ results showed that $\delta^{15}N_{AA}$ values are almost identical between the raw- and intra-OM pools (Figures 4a and 4b) and the offset between these two OM pools were rather small and overshadowed by measurement uncertainties (Figure 4c). Only Glx showed higher values in the intra-OM pool. Since inter- and intra-OM pools are concurrently formed and integrated within or wrapped around the biomineral units, we can exclude potential differences in isotopic turnover rates which cover the consumers' diet input at certain time intervals (Hebert et al., 2016; Valladares & Planas, 2012). We consider that the Glx (Gln + Glu) pool is derived either directly from the diet (unmetabolized fraction) or from the product that has gone through the metabolic procedure (metabolized fraction), for example, undergone exchange with other AAs, as Glx is known as the central product in the transamination and deamination of the rest of AAs (Cammarata & Cohen, 1950; O'Connell, 2017). The metabolized portion of Glx fractionates substantially, leading to a more enriched ^{15}N content in the residual Glx pool. However, it is difficult to attribute such a small offset in Glx to a specific metabolic process because the intrinsic fractionation and mass flux between Glx and other products (e.g., AAs) are unknown. Furthermore, relating the OM-pool-specific differences in $\delta^{15}N$ values to the relative AA amounts, it becomes clear that the large differences in the individual AA pool sizes can exaggerate the differences in their nitrogen isotope signatures. For example, Pro with a little offset in $\delta^{15}N_{intra\text{-}raw}$ values (up to 0.5‰) differed substantially in quantity (by more than 10 wt%) between the two studied OM pools, resulting in the largest contribution to the difference in BSIA-$\delta^{15}N$ values ($\delta^{15}N_{weighted\ AA}$) between intra- and raw-OM pools. However, providing a biological interpretation for this observation is challenging and beyond the scope of this study. Furthermore, although to a lesser extent (less than 30 wt%), the non-AA derived nitrogen sources, for example, glycosaminoglycans, amino sugars or nucleic acids/bases (Agbaje et al., 2019; Ferreira et al., 2020; Marxen & Becker, 1997), also contributed to the offset of $\delta^{15}N$ values between the raw- and intra-OM pools, which is of interest to quality and quantify the specific chemical components in future studies.

4.4. Future Studies

The differences in bulk and AA nitrogen isotope compositions between intra-OM and raw-OM pools of shell materials raise the question of which organic interface of bivalve shells is suitable for the reconstruction of trophic interactions among the lower positions of the food web and environmental nitrogen baseline for the modern and past oceans. Since small isotopic deviations can lead to different estimation of consumers' food sources (Michener & Kaufman, 2007), the offset of BSIA-$\delta^{15}N$ between OM pools should be considered for accurate data interpretation. For CSIA-$\delta^{15}N_{AA}$, substantially identical nitrogen isotope composition of source AAs (especially Phe) suggests the equivalent usability of both OM pools as archives to reconstruct the environmental $\delta^{15}N$ baseline. Furthermore, small differences in $\delta^{15}N_{Glx}$ values lead to small deviations of TP estimates calculated from $\delta^{15}N$ values of Glx and Phe with the $TP_{intra\text{-}OM}$ being ca. 0.6 higher than $TP_{raw\text{-}OM}$ (Figure S7 in Supporting Information S1). However, this TP difference did not exceed the propagated errors (1σ ranged from 0.4–0.6), which considered the analytical variability of $\delta^{15}N_{Glx,\ Phe}$ values and the uncertainties of trophic coefficients (β values and the trophic enrichment factors of Glx and Phe) (Bradley et al., 2015; Chikaraishi et al., 2009). Since the extraction of shell intra-OM would add enormous efforts to the already labor-intensive CSIA-$\delta^{15}N_{AA}$ procedure, these results approve the application of raw-OM at least in modern bivalve shells, which would simplify the number of sample preparation steps. Such a recommendation might not be suitable for fossil shells given the effect of diagenesis (Pérez-Huerta et al., 2020). Future studies on fossil shells using BSIA-$\delta^{15}N$ and CSIA-$\delta^{15}N_{AA}$ are needed to test the potential influences of diagenesis on the magnitude of isotopic offsets between shell OM pools. In addition, as the properties of the shell organic chemistry are linked to various factors, for example, the physiology of the bivalves and shell formation, further studies are required for an in-depth understanding of the observed isotope offsets among shell portions formed during different stages of life, between shell layers and among different bivalve species. Finally, we hope the results reported here inspire future studies to consider relevant biological processes and fundamental biomolecules when calibrating geochemical proxies of environmental variables.

5. Conclusions

The acid washing (1 N HCl) procedure for preparing shell samples (here, focusing on modern *A. islandica* shells) resulted in a loss of the ^{15}N-enriched organic component, half of which was derived from AAs that generally contained a higher proportion of trophic AAs and a lower proportion of source AAs, respectively. This led to

significantly lower BSIA-$\delta^{15}N$ values, but the decrease was very small (<0.5‰). On the other hand, acid washing produced more variable $\delta^{15}N$ data that obscured the naturally occurring isotopic distinctions between specimens. In addition, rinsing shell powders with MQ water did not alter the shell materials isotopically or chemically, showing indistinguishable BSIA-$\delta^{15}N$ values and AA compositions between the untreated shell powders and those washed with MQ water. Nevertheless, direct combustion of shell powders (<4 mg) should be preferably chosen for BSIA-$\delta^{15}N$ analysis. To extract shell intra-OM, H_2O_2 was less efficient than NaOCl. Organics extracted with H_2O_2 still contained isotope signals (both bulk and AA-specific $\delta^{15}N$) from the inter-OM. In comparison, the NaOCl oxidative cleaning protocol effectively removed the weakly bound inter-OM and generated robust bulk and AA-specific $\delta^{15}N$ data from 17 mg in case of BSIA-$\delta^{15}N$ and 500 mg of shell powder in case of CSIA-$\delta^{15}N$, respectively. Furthermore, the proportion of individual AAs differed markedly between inter- and intra-OM pools, potentially due to different formation procedures during biomineralization. This resulted in the differences in AA proportions of intra-OM and raw-OM pools, associated with different $\delta^{15}N$ values (which, however, did not differ strongly). These differences explained most of the small (ca. 0.6‰) variation of BSIA-$\delta^{15}N$ values between intra-OM and raw-OM pools. Offsets between intra-OM and raw-OM in $\delta^{15}N_{Glx}$ values were ca. 1.6‰ leading to slightly higher TP estimates in the intra-OM, but this increase was overprinted by the theoretically propagated uncertainties from the analytical methods and trophic coefficients. Balancing between the accuracy of data and the preparation efforts of samples, the raw-OM pool is sufficient for bulk and AA-specific nitrogen isotope analyses in modern bivalve shells for the purpose of reconstructing organic sources and the nitrogen isotope baseline.

Data Availability Statement

All the data generated in this study are available in the Supporting Information and are also archived via Huang, Agbaje, et al. (2023).

Acknowledgments
This project has received funding from the European Research Council under the European Union's Horizon 2020 research and innovation program (Grant agreement No 856488). We thank Michael Maus and Pascal Schmidt for laboratory support. We thank Nicolas Duprey, Frédéric Marin, Kazuyoshi Endo, Lukas Fröhlich, Hao Wu, Kirsty Penkman, Oliver Craig, and Helen Talbot for their discussions on this topic. Open Access funding enabled and organized by Projekt DEAL.

References

Addadi, L., Joester, D., Nudelman, F., & Weiner, S. (2006). Mollusk shell formation: A source of new concepts for understanding biomineralization processes. *Chemistry - A European Journal*, *12*(4), 980–987. https://doi.org/10.1002/chem.200500980

Addadi, L., & Weiner, S. (1985). Interactions between acidic proteins and crystals: Stereochemical requirements in biomineralization. *Proceedings of the National Academy of Sciences*, *82*(12), 4110–4114. https://doi.org/10.1073/pnas.82.12.4110

Agbaje, O. B. A., Ben Shir, I., Zax, D. B., Schmidt, A., & Jacob, D. E. (2018). Biomacromolecules within bivalve shells: Is chitin abundant? *Acta Biomaterialia*, *80*, 176–187. https://doi.org/10.1016/j.actbio.2018.09.009

Agbaje, O. B. A., Thomas, D. E., Dominguez, J. G., Mclnerney, B. V., Kosnik, M. A., & Jacob, D. E. (2019). Biomacromolecules in bivalve shells with crossed lamellar architecture. *Journal of Materials Science*, *54*(6), 4952–4969. https://doi.org/10.1007/s10853-018-3165-8

Agbaje, O. B. A., Thomas, D. E., Mclnerney, B. V., Molloy, M. P., & Jacob, D. E. (2017). Organic macromolecules in shells of *Arctica islandica*: Comparison with nacroprismatic bivalve shells. *Marine Biology*, *164*(11), 208. https://doi.org/10.1007/s00227-017-3238-2

Almeida, M. J., Milet, C., Peduzzi, J., Pereira, L., Haigle, J., Barthelemy, M., & Lopez, E. (2000). Effect of water-soluble matrix fraction extracted from the nacre of *Pinctada maxima* on the alkaline phosphatase activity of cultured fibroblasts. *Journal of Experimental Zoology*, *288*(4), 327–334. https://doi.org/10.1002/1097-010X(20001215)288:4<327::AID-JEZ5>3.0.CO;2

Anderson, M., & Braak, C. T. (2003). Permutation tests for multi-factorial analysis of variance. *Journal of Statistical Computation and Simulation*, *73*(2), 85–113. https://doi.org/10.1080/00949650215733

Arias, J. L., & Fernández, M. S. (2008). Polysaccharides and proteoglycans in calcium carbonate-based biomineralization. *Chemical Reviews*, *108*(11), 4475–4482. https://doi.org/10.1021/cr078269p

Bada, J. L., Schoeninger, M. J., & Schimmelmann, A. (1989). Isotopic fractionation during peptide bond hydrolysis. *Geochimica et Cosmochimica Acta*, *53*(12), 3337–3341. https://doi.org/10.1016/0016-7037(89)90114-2

Bada, J. L., Shou, M.-Y., Man, E. H., & Schroeder, R. A. (1978). Decomposition of hydroxy amino acids in foraminiferal tests; kinetics, mechanism and geochronological implications. *Earth and Planetary Science Letters*, *41*(1), 67–76. https://doi.org/10.1016/0012-821X(78)90042-0

Bates, D., Kliegl, R., Vasishth, S., & Baayen, H. (2015). Parsimonious mixed models. ArXiv Preprint ArXiv:1506.04967.

Black, H. D., Andrus, C. F. T., Lambert, W. J., Rick, T. C., & Gillikin, D. P. (2017). $\delta^{15}N$ values in *Crassostrea virginica* shells provides early direct evidence for nitrogen loading to Chesapeake Bay. *Scientific Reports*, *7*(1), 44241. https://doi.org/10.1038/srep44241

Borukhin, S., Bloch, L., Radlauer, T., Hill, A. H., Fitch, A. N., & Pokroy, B. (2012). Screening the incorporation of amino acids into an inorganic crystalline host: The case of calcite. *Advanced Functional Materials*, *22*(20), 4216–4224. https://doi.org/10.1002/adfm.201201079

Bowen, C. E., & Tang, H. (1996). Conchiolin-protein in aragonite shells of mollusks. *Comparative Biochemistry and Physiology Part A: Physiology*, *115*(4), 269–275. https://doi.org/10.1016/S0300-9629(96)00059-X

Bradley, C. J., Wallsgrove, N. J., Choy, C. A., Drazen, J. C., Hetherington, E. D., Hoen, D. K., & Popp, B. N. (2015). Trophic position estimates of marine teleosts using amino acid compound specific isotopic analysis: Stable isotope-derived trophic positions of teleosts. *Limnology and Oceanography: Methods*, *13*(9), 476–493. https://doi.org/10.1002/lom3.10041

Brault, E. K., Koch, P. L., Gier, E., Ruiz-Cooley, R. I., Zupcic, J., Gilbert, K. N., & McCarthy, M. D. (2014). Effects of decalcification on bulk and compound-specific nitrogen and carbon isotope analyses of dentin: Effects of decalcification on isotope analyses of dentin. *Rapid Communications in Mass Spectrometry*, *28*(24), 2744–2752. https://doi.org/10.1002/rcm.7073

Cammarata, P. S., & Cohen, P. P. (1950). The scope of the transamination reaction in animal tissues. *Journal of Biological Chemistry*, *187*(1), 439–452. https://doi.org/10.1016/s0021-9258(19)50969-3

Carmichael, R., Hattenrath, T., Valiela, I., & Michener, R. (2008). Nitrogen stable isotopes in the shell of *Mercenaria mercenaria* trace wastewater inputs from watersheds to estuarine ecosystems. *Aquatic Biology*, *4*, 99–111. https://doi.org/10.3354/ab00106

Carter, J. G. (Ed.). (1990). *Skeletal biomineralization: Patterns, processes, and evolutionary trends* (Vol. 1). Van Nostrand Reinhold.
Caut, S., Angulo, E., & Courchamp, F. (2009). Variation in discrimination factors ($\Delta^{15}N$ and $\Delta^{13}C$): The effect of diet isotopic values and applications for diet reconstruction. *Journal of Applied Ecology*, *46*(2), 443–453. https://doi.org/10.1111/j.1365-2664.2009.01620.x
Chikaraishi, Y., Kashiyama, Y., Ogawa, N., Kitazato, H., & Ohkouchi, N. (2007). Metabolic control of nitrogen isotope composition of amino acids in macroalgae and gastropods: Implications for aquatic food web studies. *Marine Ecology Progress Series*, *342*, 85–90. https://doi.org/10.3354/meps342085
Chikaraishi, Y., Ogawa, N. O., Kashiyama, Y., Takano, Y., Suga, H., Tomitani, A., et al. (2009). Determination of aquatic food-web structure based on compound-specific nitrogen isotopic composition of amino acids: Trophic level estimation by amino acid $\delta^{15}N$. *Limnology and Oceanography: Methods*, *7*(11), 740–750. https://doi.org/10.4319/lom.2009.7.740
Currey, J. D., & Taylor, J. D. (1974). The mechanical behaviour of some molluscan hard tissues. *Journal of Zoology*, *173*(3), 395–406. https://doi.org/10.1111/j.1469-7998.1974.tb04122.x
Darrow, E. S., Carmichael, R. H., Andrus, C. F. T., & Jackson, H. E. (2017). From middens to modern estuaries, oyster shells sequester source-specific nitrogen. *Geochimica et Cosmochimica Acta*, *202*, 39–56. https://doi.org/10.1016/j.gca.2016.12.023
Das, S., Judd, E. J., Uveges, B. T., Ivany, L. C., & Junium, C. K. (2021). Variation in $\delta^{15}N$ from shell-associated organic matter in bivalves: Implications for studies of modern and fossil ecosystems. *Palaeogeography, Palaeoclimatology, Palaeoecology*, *562*, 110076. https://doi.org/10.1016/j.palaeo.2020.110076
Demarchi, B., Clements, E., Coltorti, M., van de Locht, R., Kröger, R., Penkman, K., & Rose, J. (2015). Testing the effect of bleaching on the bivalve *Glycymeris*: A case study of amino acid geochronology on key Mediterranean raised beach deposits. *Quaternary Geochronology*, *25*, 49–65. https://doi.org/10.1016/j.quageo.2014.09.003
Demarchi, B., Rogers, K., Fa, D. A., Finlayson, C. J., Milner, N., & Penkman, K. (2013). Intra-crystalline protein diagenesis (IcPD) in *Patella vulgata*. Part I: Isolation and testing of the closed system. *Quaternary Geochronology*, *16*, 144–157. https://doi.org/10.1016/j.quageo.2012.03.016
Deng, Z., Jia, Z., & Li, L. (2022). Biomineralized materials as model systems for structural composites: Intracrystalline structural features and their strengthening and toughening mechanisms. *Advanced Science*, *9*(14), 2103524. https://doi.org/10.1002/advs.202103524
Deniro, M. J., & Epstein, S. (1981). Influence of diet on the distribution of nitrogen isotopes in animals. *Geochimica et Cosmochimica Acta*, *45*(3), 341–351. https://doi.org/10.1016/0016-7037(81)90244-1
Denis, A. (1972). *Essai sur la microstructure du test de lamellibranches*. Travaux du Laboratoire de Paleontologie, Universitd de Paris, Facultd des Sciences d'Orsay.
Ellis, G. S. (2012). *Compound-specific stable isotopic analysis of protein amino acids: Ecological applications in modern and ancient systems* (Doctoral dissertation). University of South Florida. Retrieved from https://digitalcommons.usf.edu/etd/4035
Fantle, M. S., Dittel, A. I., Schwalm, S. M., Epifanio, C. E., & Fogel, M. L. (1999). A food web analysis of the juvenile blue crab, *Callinectes sapidus*, using stable isotopes in whole animals and individual amino acids. *Oecologia*, *120*(3), 416–426. https://doi.org/10.1007/s004420050874
Ferreira, S., Ashby, R., Jeunen, G. J., Rutherford, K., Collins, C., Todd, E. V., & Gemmell, N. J. (2020). DNA from mollusc shell: A valuable and underutilised substrate for genetic analyses. *PeerJ*, *8*, e9420. https://doi.org/10.7717/peerj.9420
Fichtner, V., Strauss, H., Immenhauser, A., Buhl, D., Neuser, R. D., & Niedermayr, A. (2017). Diagenesis of carbonate associated sulfate. *Chemical Geology*, *463*, 61–75. https://doi.org/10.1016/j.chemgeo.2017.05.008
Fox, J., & Weisberg, S. (2019). *An R companion to applied regression* (3rd ed.). Sage. Retrieved from https://socialsciences.mcmaster.ca/jfox/Books/Companion/
Fry, B. (2006). *Stable isotope ecology*. Springer.
Gaffey, S. J., & Bronnimann, C. E. (1993). Effects of bleaching on organic and mineral phases in biogenic carbonates. *Journal of Sedimentary Research*, *63*(4), 752–754. https://doi.org/10.1306/d4267be0-2b26-11d7-8648000102c1865d
Germain, L., Koch, P., Harvey, J., & McCarthy, M. (2013). Nitrogen isotope fractionation in amino acids from harbor seals: Implications for compound-specific trophic position calculations. *Marine Ecology Progress Series*, *482*, 265–277. https://doi.org/10.3354/meps10257
Gilbert, P., Bergmann, K. D., Boekelheide, N., Tambutté, S., Mass, T., Marin, F., et al. (2022). Biomineralization: Integrating mechanism and evolutionary history. *Science Advances*, *8*(10), eabl9653. https://doi.org/10.1126/sciadv.abl9653
Giuffre, A. J., Hamm, L. M., Han, N., De Yoreo, J. J., & Dove, P. M. (2013). Polysaccharide chemistry regulates kinetics of calcite nucleation through competition of interfacial energies. *Proceedings of the National Academy of Sciences*, *110*(23), 9261–9266. https://doi.org/10.1073/pnas.1222162110
Gotliv, B.-A., Addadi, L., & Weiner, S. (2003). Mollusk shell acidic proteins: In search of individual functions. *ChemBioChem*, *4*(6), 522–529. https://doi.org/10.1002/cbic.200200548
Graniero, L. E., Gillikin, D. P., Surge, D., Kelemen, Z., & Bouillon, S. (2021). Assessing $\delta^{15}N$ values in the carbonate-bound organic matrix and periostracum of bivalve shells as environmental archives. *Palaeogeography, Palaeoclimatology, Palaeoecology*, *564*, 110108. https://doi.org/10.1016/j.palaeo.2020.110108
Graniero, L. E., Grossman, E. L., & O'Dea, A. (2016). Stable isotopes in bivalves as indicators of nutrient source in coastal waters in the Bocas del Toro Archipelago, Panama. *PeerJ*, *4*, e2278. https://doi.org/10.7717/peerj.2278
Hare, E. P., Fogel, M. L., Stafford, T. W., Mitchell, A. D., & Hoering, T. C. (1991). The isotopic composition of carbon and nitrogen in individual amino acids isolated from modern and fossil proteins. *Journal of Archaeological Science*, *18*(3), 277–292. https://doi.org/10.1016/0305-4403(91)90066-X
Hebert, C. E., Popp, B. N., Fernie, K. J., Ka'apu-Lyons, C., Rattner, B. A., & Wallsgrove, N. (2016). Amino acid specific stable nitrogen isotope values in avian tissues: Insights from captive American kestrels and wild herring gulls. *Environmental Science & Technology*, *50*(23), 12928–12937. https://doi.org/10.1021/acs.est.6b04407
Hovden, R., Wolf, S. E., Holtz, M. E., Marin, F., Muller, D. A., & Estroff, L. A. (2015). Nanoscale assembly processes revealed in the nacroprismatic transition zone of *Pinna nobilis* mollusc shells. *Nature Communications*, *6*(1), 10097. https://doi.org/10.1038/ncomms10097
Huang, Q., Agbaje, O. B. A., Conti, M., & Schöne, B. R. (2023). Supplementary data to: "Organic phases in bivalve (*Arctica islandica*) shells: Their bulk and amino acid nitrogen stable isotope compositions" in Geochemistry, Geophysics, Geosystems (Version 1). [Dataset]. Zenodo. https://doi.org/10.5281/zenodo.8425303
Huang, Q., Wu, H., & Schöne, B. R. (2023). A novel trophic archive: Practical considerations of compound-specific amino acid $\delta^{15}N$ analysis of carbonate-bound organic matter in bivalve shells (*Arctica islandica*). *Chemical Geology*, *615*, 121220. https://doi.org/10.1016/j.chemgeo.2022.121220
Kassambara, A., & Mundt, F. (2017). Factoextra: Extract and visualize the results of multivariate data analyses. *R Package Version*, *1*(5), 337–354.
Kovacs, C., Daskin, J., Patterson, H., & Carmichael, R. (2010). *Crassostrea virginica* shells record local variation in wastewater inputs to a coastal estuary. *Aquatic Biology*, *9*, 77–84. https://doi.org/10.3354/ab00228

Kuznetsova, A., Brockhoff, P. B., & Christensen, R. H. B. (2017). lmerTest package: Tests in linear mixed effects models. *Journal of Statistical Software*, *82*(13), 1–26. https://doi.org/10.18637/jss.v082.i13

Li, L., Weaver, J. C., & Ortiz, C. (2015). Hierarchical structural design for fracture resistance in the shell of the pteropod *Clio pyramidata*. *Nature Communications*, *6*(1), 6216. https://doi.org/10.1038/ncomms7216

Lueders-Dumont, J. A., Wang, X. T., Jensen, O. P., Sigman, D. M., & Ward, B. B. (2018). Nitrogen isotopic analysis of carbonate-bound organic matter in modern and fossil fish otoliths. *Geochimica et Cosmochimica Acta*, *224*, 200–222. https://doi.org/10.1016/j.gca.2018.01.001

Macko, S. A., Estep, M. L. F., Engel, M. H., & Hare, P. E. (1986). Kinetic fractionation of stable nitrogen isotopes during amino acid transamination. *Geochimica et Cosmochimica Acta*, *50*(10), 2143–2146. https://doi.org/10.1016/0016-7037(86)90068-2

Mann, S. (2001). *Biomineralization: Principles and concepts in bioinorganic materials chemistry*. Oxford University Press.

Marali, S., Schöne, B. R., Mertz-Kraus, R., Griffin, S. M., Wanamaker, A. D., Matras, U., & Butler, P. G. (2017). Ba/Ca ratios in shells of *Arctica islandica*—Potential environmental proxy and crossdating tool. *Palaeogeography, Palaeoclimatology, Palaeoecology*, *465*, 347–361. https://doi.org/10.1016/j.palaeo.2015.12.018

Marie, B., Luquet, G., Pais De Barros, J.-P., Guichard, N., Morel, S., Alcaraz, G., et al. (2007). The shell matrix of the freshwater mussel *Unio pictorum* (Paleoheterodonta, Unionoida): Involvement of acidic polysaccharides from glycoproteins in nacre mineralization. *FEBS Journal*, *274*(11), 2933–2945. https://doi.org/10.1111/j.1742-4658.2007.05825.x

Marie, B., Ramos-Silva, P., Marin, F., & Marie, A. (2013). Proteomics of $CaCO_3$ biomineral-associated proteins: How to properly address their analysis. *Proteomics*, *13*(21), 3109–3116. https://doi.org/10.1002/pmic.201300162

Marin, F., & Luquet, G. (2004). Molluscan shell proteins. *Comptes Rendus Palevol*, *3*(6–7), 469–492. https://doi.org/10.1016/j.crpv.2004.07.009

Marin, F., Luquet, G., Marie, B., & Medakovic, D. (2007). Molluscan shell proteins: Primary structure, origin, and evolution. In *Current topics in developmental biology* (Vol. 80, pp. 209–276). Elsevier. https://doi.org/10.1016/S0070-2153(07)80006-8

Martinez Arbizu, P. (2019). pairwiseAdonis: pairwise multilevel comparison using adonis – R package ver. 0.3.

Martínez-García, A., Jung, J., Ai, X. E., Sigman, D. M., Auderset, A., Duprey, N. N., et al. (2022). Laboratory assessment of the impact of chemical oxidation, mineral dissolution, and heating on the nitrogen isotopic composition of fossil-bound organic matter. *Geochemistry, Geophysics, Geosystems*, *23*(8), e2022GC010396. https://doi.org/10.1029/2022GC010396

Marxen, J. C., & Becker, W. (1997). The organic shell matrix of the freshwater snail *Biomphalaria glabrata*. *Comparative Biochemistry and Physiology Part B: Biochemistry and Molecular Biology*, *118*(1), 23–33. https://doi.org/10.1016/S0305-0491(97)00010-2

Mateo, M. A., Serrano, O., Serrano, L., & Michener, R. H. (2008). Effects of sample preparation on stable isotope ratios of carbon and nitrogen in marine invertebrates: Implications for food web studies using stable isotopes. *Oecologia*, *157*(1), 105–115. https://doi.org/10.1007/s00442-008-1052-8

McClelland, J. W., & Montoya, J. P. (2002). Trophic relationships and the nitrogen isotopic composition of amino acids in plankton. *Ecology*, *83*(8), 2173–2180. https://doi.org/10.1890/0012-9658(2002)083[2173:TRATNI]2.0.CO;2

Meckler, A. N., Schubert, C. J., Hochuli, P. A., Plessen, B., Birgel, D., Flower, B. P., et al. (2008). Glacial to Holocene terrigenous organic matter input to sediments from Orca Basin, Gulf of Mexico—A combined optical and biomarker approach. *Earth and Planetary Science Letters*, *272*(1–2), 251–263. https://doi.org/10.1016/j.epsl.2008.04.046

Meenakshi, V. R., Blackwelder, P. L., & Wilbur, K. M. (1973). An ultrastructural study of shell regeneration in *Mytilus edulis* (Mollusca: Bivalvia). *Journal of Zoology*, *171*(4), 475–484. https://doi.org/10.1111/j.1469-7998.1973.tb02229.x

Meldrum, F. C., & Cölfen, H. (2008). Controlling mineral morphologies and structures in biological and synthetic systems. *Chemical Reviews*, *108*(11), 4332–4432. https://doi.org/10.1021/cr8002856

Michener, R. H., & Kaufman, L. (2007). Stable isotope ratios as tracers in marine food webs: An update. In R. Michener & K. Lajtha (Eds.), *Stable isotopes in ecology and environmental science* (pp. 238–282). Blackwell Publishing Ltd.

Michenfelder, M., Fu, G., Lawrence, C., Weaver, J. C., Wustman, B. A., Taranto, L., et al. (2003). Characterization of two molluscan crystal-modulating biomineralization proteins and identification of putative mineral binding domains. *Biopolymers*, *70*(4), 522–533. https://doi.org/10.1002/bip.10536

Milano, S., Schöne, B. R., & Gutiérrez-Zugasti, I. (2020). Oxygen and carbon stable isotopes of *Mytilus galloprovincialis* Lamarck, 1819 shells as environmental and provenance proxies. *The Holocene*, *30*(1), 65–76. https://doi.org/10.1177/0959683619865595

Minagawa, M., & Wada, E. (1984). Stepwise enrichment of ^{15}N along food chains: Further evidence and the relation between $\delta^{15}N$ and animal age. *Geochimica et Cosmochimica Acta*, *48*(5), 1135–1140. https://doi.org/10.1016/0016-7037(84)90204-7

Misarti, N., Gier, E., Finney, B., Barnes, K., & McCarthy, M. (2017). Compound-specific amino acid $\delta^{15}N$ values in archaeological shell: Assessing diagenetic integrity and potential for isotopic baseline reconstruction. *Rapid Communications in Mass Spectrometry*, *31*(22), 1881–1891. https://doi.org/10.1002/rcm.7963

Newell, R. (2004). Ecosystem influences of natural and cultivated populations of suspension-feeding bivalve molluscs: A review. *Journal of Shellfish Research*, *23*(1), 51–61.

Nudelman, F., Chen, H. H., Goldberg, H. A., Weiner, S., & Addadi, L. (2007). Lessons from biomineralization: Comparing the growth strategies of mollusc shell prismatic and nacreous layers in *Atrina rigida*. *Faraday Discussions*, *136*, 9. https://doi.org/10.1039/b704418f

O'Connell, T. C. (2017). 'Trophic' and 'source' amino acids in trophic estimation: A likely metabolic explanation. *Oecologia*, *184*(2), 317–326. https://doi.org/10.1007/s00442-017-3881-9

Oczkowski, A., Gumbley, T., Carter, B., Carmichael, R., & Humphries, A. (2016). Establishing an anthropogenic nitrogen baseline using native American shell middens. *Frontiers in Marine Science*, *3*, 79. https://doi.org/10.3389/fmars.2016.00079

O'Donnell, T. H., Macko, S. A., Chou, J., Davis-Hartten, K. L., & Wehmiller, J. F. (2003). Analysis of $\delta^{13}C$, $\delta^{15}N$, and $\delta^{34}S$ in organic matter from the biominerals of modern and fossil *Mercenaria* spp. *Organic Geochemistry*, *34*(2), 165–183. https://doi.org/10.1016/S0146-6380(02)00160-2

Ohkouchi, N., Chikaraishi, Y., Close, H. G., Fry, B., Larsen, T., Madigan, D. J., et al. (2017). Advances in the application of amino acid nitrogen isotopic analysis in ecological and biogeochemical studies. *Organic Geochemistry*, *113*, 150–174. https://doi.org/10.1016/j.orggeochem.2017.07.009

Oksanen, J., Kindt, R., Simpson, G. L., & Oksanen, M. J. (2018). Package 'vegan3d.' R package version, 1–0.

Okumura, T., Suzuki, M., Nagasawa, H., & Kogure, T. (2013). Microstructural control of calcite via incorporation of intracrystalline organic molecules in shells. *Journal of Crystal Growth*, *381*, 114–120. https://doi.org/10.1016/j.jcrysgro.2013.07.020

Ortiz, J. E., Gutiérrez-Zugasti, I., Torres, T., González-Morales, M., & Sánchez-Palencia, Y. (2015). Protein diagenesis in Patella shells: Implications for amino acid racemisation dating. *Quaternary Geochronology*, *27*, 105–118. https://doi.org/10.1016/j.quageo.2015.02.008

Pape, E., Gill, F. L., Newton, R. J., Little, C. T. S., & Abbott, G. D. (2018). Methodological comparison for the isolation of shell-bound organic matter for carbon, nitrogen and sulfur stable isotope analysis. *Chemical Geology*, *493*, 87–99. https://doi.org/10.1016/j.chemgeo.2018.05.028

Pardieck, D. L., Bouwer, E. J., & Stone, A. T. (1992). Hydrogen peroxide use to increase oxidant capacity for in situ bioremediation of contaminated soils and aquifers: A review. *Journal of Contaminant Hydrology*, *9*(3), 221–242. https://doi.org/10.1016/0169-7722(92)90006-Z

Penkman, K. (2009). Amino acid geochronology: Its impact on our understanding of the Quaternary stratigraphy of the British Isles. *Journal of Quaternary Science*, *25*(4), 501–514. https://doi.org/10.1002/jqs.1346

Penkman, K., Kaufman, D. S., Maddy, D., & Collins, M. J. (2008). Closed-system behaviour of the intra-crystalline fraction of amino acids in mollusc shells. *Quaternary Geochronology*, *3*(1–2), 2–25. https://doi.org/10.1016/j.quageo.2007.07.001

Pereira-Mouriès, L., Almeida, M.-J., Ribeiro, C., Peduzzi, J., Barthélemy, M., Milet, C., & Lopez, E. (2002). Soluble silk-like organic matrix in the nacreous layer of the bivalve *Pinctada maxima*: A new insight in the biomineralization field. *European Journal of Biochemistry*, *269*(20), 4994–5003. https://doi.org/10.1046/j.1432-1033.2002.03203.x

Pérez-Huerta, A., Walker, S. E., & Cappelli, C. (2020). In situ geochemical analysis of organics in growth lines of Antarctic scallop shells: Implications for sclerochronology. *Minerals*, *10*(6), 529. https://doi.org/10.3390/min10060529

Polissar, P. J., Fulton, J. M., Junium, C. K., Turich, C. C., & Freeman, K. H. (2009). Measurement of ^{13}C and ^{15}N isotopic composition on nanomolar quantities of C and N. *Analytical Chemistry*, *81*(2), 755–763. https://doi.org/10.1021/ac801370c

Popov, S. V. (1986). Composite prismatic structure in bivalve shell. *Acta Palaeontologica Polonica*, *31*(1–2), 3–26.

Popp, B. N., Graham, B. S., Olson, R. J., Hannides, C. C. S., Lott, M. J., López-Ibarra, G. A., et al. (2007). Insight into the trophic ecology of yellowfin tuna, *Thunnus albacares*, from compound-specific nitrogen isotope analysis of proteinaceous amino acids. *Terrestrial Ecology*, *1*, 173–190. https://doi.org/10.1016/S1936-7961(07)01012-3

Post, D. M. (2002). Using stable isotopes to estimate trophic position: Models, methods, and assumptions. *Ecology*, *83*(3), 703–718. https://doi.org/10.1890/0012-9658(2002)083[0703:USITET]2.0.CO;2

R Core Team. (2021). *R: A language and environment for statistical computing*. R Foundation for Statistical Computing. Retrieved from https://www.R-project.org/

Rhoads, D. C., & Lutz, R. A. (1980). *Skeletal growth of aquatic organisms: Biological records of environmental change* (Vol. 1). Plenum Press.

Richardson, C. A. (2001). Molluscs as archives of environmental change. *Oceanography and Marine Biology an Annual Review*, *39*, 103–164.

Riès-kautt, M., & Ducruix, A. (1997). [3] Inferences drawn from physicochemical studies of crystallogenesis and precrystalline state. *Methods in Enzymology*, *276*, 23–59. https://doi.org/10.1016/S0076-6879(97)76049-X

Robinson, R. S., Kienast, M., Luiza Albuquerque, A., Altabet, M., Contreras, S., De Pol Holz, R., et al. (2012). A review of nitrogen isotopic alteration in marine sediments. *Paleoceanography and Paleoclimatology*, *27*(4). https://doi.org/10.1029/2012PA002321

Ropes, J. W., Jones, D. S., Murawski, S. A., Serchuk, F. M., & Jearld, A., Jr. (1984). Documentation of annual growth lines in ocean quahogs, *Arctica islandica* Linné. *Fishery Bulletin*, *82*(1), 1.

Schlacher, T. A., & Connolly, R. M. (2014). Effects of acid treatment on carbon and nitrogen stable isotope ratios in ecological samples: A review and synthesis. *Methods in Ecology and Evolution*, *5*(6), 541–550. https://doi.org/10.1111/2041-210X.12183

Schöne, B. R. (2013). *Arctica islandica* (Bivalvia): A unique paleoenvironmental archive of the northern North Atlantic Ocean. *Global and Planetary Change*, *111*, 199–225. https://doi.org/10.1016/j.gloplacha.2013.09.013

Schöne, B. R., & Huang, Q. (2021). Ontogenetic $\delta^{15}N$ trends and multidecadal variability in shells of the bivalve mollusk, *Arctica islandica*. *Frontiers in Marine Science*, *8*, 748593. https://doi.org/10.3389/fmars.2021.748593

Schubert, C. J., & Calvert, S. E. (2001). Nitrogen and carbon isotopic composition of marine and terrestrial organic matter in Arctic Ocean sediments. *Deep Sea Research Part I: Oceanographic Research Papers*, *48*(3), 789–810. https://doi.org/10.1016/S0967-0637(00)00069-8

Seuront, L., & Spilmont, N. (2002). Self-organized criticality in intertidal microphytobenthos patch patterns. *Physica A: Statistical Mechanics and its Applications*, *313*(3–4), 513–539. https://doi.org/10.1016/S0378-4371(02)00989-5

Silfer, J. A., Engel, M. H., & Macko, S. A. (1992). Kinetic fractionation of stable carbon and nitrogen isotopes during peptide bond hydrolysis: Experimental evidence and geochemical implications. *Chemical Geology: Isotope Geoscience section*, *101*(3–4), 211–221. https://doi.org/10.1016/0009-2541(92)90003-N

Steinhardt, J., Butler, P. G., Carroll, M. L., & Hartley, J. (2016). The application of long-lived bivalve sclerochronology in environmental baseline monitoring. *Frontiers in Marine Science*, *3*, 176. https://doi.org/10.3389/fmars.2016.00176

Styring, A. K., Kuhl, A., Knowles, T. D. J., Fraser, R. A., Bogaard, A., & Evershed, R. P. (2012). Practical considerations in the determination of compound-specific amino acid $\delta^{15}N$ values in animal and plant tissues by gas chromatography-combustion-isotope ratio mass spectrometry, following derivatisation to their *N* -acetylisopropyl esters: Determining AA δ^{15} N values by GC-C-IRMS. *Rapid Communications in Mass Spectrometry*, *26*(19), 2328–2334. https://doi.org/10.1002/rcm.6322

Sykes, G. A., Collins, M. J., & Walton, D. I. (1995). The significance of a geochemically isolated intracrystalline organic fraction within biominerals. *Organic Geochemistry*, *23*(11–12), 1059–1065. https://doi.org/10.1016/0146-6380(95)00086-0

Takano, Y., Kashiyama, Y., Ogawa, N. O., Chikaraishi, Y., & Ohkouchi, N. (2010). Isolation and desalting with cation-exchange chromatography for compound-specific nitrogen isotope analysis of amino acids: Application to biogeochemical samples: Compound-specific nitrogen isotope analysis of amino acids. *Rapid Communications in Mass Spectrometry*, *24*(16), 2317–2323. https://doi.org/10.1002/rcm.4651

Tseng, H.-C., Lee, C.-Y., Weng, W.-L., & Shiah, I.-M. (2009). Solubilities of amino acids in water at various pH values under 298.15K. *Fluid Phase Equilibria*, *285*(1–2), 90–95. https://doi.org/10.1016/j.fluid.2009.07.017

Valladares, S., & Planas, M. (2012). Non-lethal dorsal fin sampling for stable isotope analysis in seahorses. *Aquatic Ecology*, *46*(3), 363–370. https://doi.org/10.1007/s10452-012-9407-y

Versteegh, E. A. A., Gillikin, D. P., & Dehairs, F. (2011). Analysis of δ^{15} N values in mollusk shell organic matrix by elemental analysis/isotope ratio mass spectrometry without acidification: An evaluation and effects of long-term preservation. *Rapid Communications in Mass Spectrometry*, *25*(5), 675–680. https://doi.org/10.1002/rcm.4905

Vizzini, S., & Mazzola, A. (2003). Seasonal variations in the stable carbon and nitrogen isotope ratios ($^{13}C/^{12}C$ and $^{15}N/^{14}N$) of primary producers and consumers in a western Mediterranean coastal lagoon. *Marine Biology*, *142*(5), 1009–1018. https://doi.org/10.1007/s00227-003-1027-6

Vokhshoori, N. L., Tipple, B. J., Teague, L., Bailess, A., & McCarthy, M. D. (2022). Calibrating bulk and amino acid $\delta^{13}C$ and $\delta^{15}N$ isotope ratios between bivalve soft tissue and shell for paleoecological reconstructions. *Palaeogeography, Palaeoclimatology, Palaeoecology*, *595*, 110979. https://doi.org/10.1016/j.palaeo.2022.110979

Wang, X. T., Sigman, D. M., Cohen, A. L., Sinclair, D. J., Sherrell, R. M., Weigand, M. A., et al. (2015). Isotopic composition of skeleton-bound organic nitrogen in reef-building symbiotic corals: A new method and proxy evaluation at Bermuda. *Geochimica et Cosmochimica Acta*, *148*, 179–190. https://doi.org/10.1016/j.gca.2014.09.017

Watanabe, S., Kodama, M., & Fukuda, M. (2009). Nitrogen stable isotope ratio in the manila clam, *Ruditapes philippinarum*, reflects eutrophication levels in tidal flats. *Marine Pollution Bulletin*, *58*(10), 1447–1453. https://doi.org/10.1016/j.marpolbul.2009.06.018

Weiner, S., & Addadi, L. (1997). Design strategies in mineralized biological materials. *Journal of Materials Chemistry*, *7*(5), 689–702. https://doi.org/10.1039/a604512j